

Large-Scale Rate-Splitting Multiple Access in Uplink UAV Networks: Effective Secrecy Throughput Maximization Under Limited Feedback Channel

Hamed Bastami, Hamid Behroozi, *Member, IEEE*, Majid Moradikia, Ahmed Abdelhadi, Derrick Wing Kwan Ngand, *Fellow, IEEE*, and Lajos Hanzo, *Life Fellow, IEEE*

Abstract—Unmanned aerial vehicles (UAVs) are capable of improving the performance of next generation wireless systems. Specifically, UAVs can be exploited as aerial base-stations (UAV-BS) for supporting legitimate ground users in remote uncovered areas or in environments temporarily requiring high capacity. However, their communication performance is prone to both channel estimation errors and potential eavesdropping. Hence, we investigate the effective secrecy throughput of the UAV-aided uplink, in which rate-splitting multiple access (RSMA) is employed by each legitimate user for secure transmission under the scenario of massive access. To maximize the effective network secrecy throughput in the uplink, the transmission rate vs. power allocation relationship is formulated as a max-min optimization problem, relying on realistic imperfect channel state information (CSI) of both the legitimate users and of the potential eavesdroppers (*Eves*). We then propose a novel transformation of the associated probabilistic constraints for decoupling the variables, so that our design problem can be solved by alternatively activating the related block coordinate decent programming. In the model considered, each user transmits a superposition of two messages to a UAV-BS, each having different transmit power and the UAV-BS uses a successive interference cancellation (SIC) technique to decode the received messages. Given the non-convexity of the problem, it is decoupled into a pair of sub-problems. In particular, we derive a closed form expression for the optimal rate-splitting fraction of each user. Then, given the optimal

rate-splitting fraction of each user, the ϵ -constrained transmit power of each user is calculated by harnessing sequential parametric convex approximation (SPCA) programming. Finally, the optimal SIC order is determined by an exhaustive search method. Our simulation results confirm that the scheme conceived significantly improves the effective secrecy throughput compared to both the existing orthogonal and non-orthogonal benchmarks as well as to the RSMA scheme ignoring CSI uncertainty.

Index Terms—Rate-splitting, physical layer security, effective network secrecy throughput, imperfect CSIT, connection outage probability, secrecy outage probability, worst-case optimization, uplink UAV networks.

I. INTRODUCTION

IN order to support the emerging Beyond 5G (B5G) system concept, unmanned aerial vehicles (UAV) may be harnessed as air-borne base-station (BS), particularly in areas of high tele-traffic density [1]-[6]. However, owing to their LoS propagation UAV-BSs usually suffer from strong co-channel interference. Although this problem can be potentially mitigated by the sophisticated trajectory design of UAVs [1], [2], the degree of freedom attained is typically inadequate to support the ever-growing terrestrial user population. In this context, multiple access (MA) techniques play a crucial role in fulfilling the high data rate, low latency, and massive connectivity requirements, as the three most important Key Performance Indicators (KPI)s for B5G [3]-[13].

Rate-splitting multiple access (RSMA) has attracted a great deal of interest, as a key-enabling radio access technology capable of satisfying the massive connectivity requirements of B5G [3], [5], [6], [9]-[13]. Briefly, RSMA is a generalization of

Hamed Bastami and Hamid Behroozi are with the Department of Electrical Engineering, Sharif University of Technology, Tehran, Iran, e-mails: {hamed.bastami@ee., behroozi@}sharif.edu

Majid Moradikia is with Department of Data Science Worcester Polytechnic Institute, Worcester, Massachusetts, e-mail: {mmoradikia@wpi.edu}. Ahmed Abdelhadi is with the Engineering Technology Department at University of Houston, e-mails: {aabdelhadi}@uh.edu.

Derrick Wing Kwan N is with the School of Electrical Engineering and Telecommunications, University of New South Wales, Sydney, Australia, e-mail: w.k.ng@unsw.edu.au.

Lajos Hanzo is with the University of Southampton, Southampton SO17 1BJ, U.K, e-mail: hanzo@soton.ac.uk.

non-orthogonal multiple access (NOMA) and space-division multiple access (SDMA) [9], that outperforms both schemes in terms of its robustness and spectral efficiency. In a rate-splitting (RS) scheme, the transmitted signals are split into two parts at the transmitter (Tx), namely into a common message and a private message. Subsequently, by performing successive interference cancellation (SIC) at the receiver (Rx), the capacity region of the MA channel (MAC) can be approached. Inspired by this promising MA framework, most of the RSMA-based literature considered the downlink (DL) [3], [5], [6], [9], [10] even though the DL actually represents a broadcast scenario and multiple access is only possible in the uplink (UL). In [11] a RS scheme was designed for guaranteeing max-min fairness in UL-NOMA. As a further advance, a cooperative rate-splitting (CRS) UL scheme was proposed in [12], where each user broadcasts his/her signal during the first phase and receives the transmitted signal of the other user, while during the second phase, each user relays the other user's message. Then, Yang *et al.* [13], proposed UL-RSMA for maximizing the users' sum-rate sum-rate by optimally sharing the total transmit powers of both user-messages, while exhaustively searching for the optimal decoding order at the SIC receiver. However, these contributions stipulate the idealized simplifying assumption of having perfect channel state information (CSI) for resource allocation design, which is not realistic in practice. More particularly, in massive access scenarios in which a large number of CSIs have to be reported to the BS using limited feedback having CSI imperfections is unavoidable, resulting in link outage [8], [14]. More importantly, none of the above-mentioned RSMA UL scenarios of [11]-[13] have addressed the associated security concerns. In particular, the concurrent UL transmissions of a massive number of messages over the same bandwidth increases the risk of security breaches. To protect the confidentiality of the transmitted signals, physical layer security (PLS) techniques can be exploited for increasing the channel capacity difference between the legitimate and eavesdropping links. Unfortunately, MA systems are particularly susceptible to passive attacks, since the eavesdroppers (*Eves*) have more target users, they can glean information from [5], [8], [10]. In this context, jamming aims for confusing the potential *Eves* by deliberately injecting specifically designed artificial

noise (AN) with the aid of beamforming [15], [16]. As a further development, the authors of [17], [18] proposed a secure NOMA approach. However, since the super-imposed non-orthogonal signals may be detected by SIC at *Eve*, superposition potentially degrades the level of security. In fact, after detecting the superimposed streams *Eve* becomes capable of wiretapping the rest of the embedded information, which is becoming less interference-infested. By contrast, using an RSMA scheme, the common message plays the dual roles of the desired message as well as that of the AN without the need for assigning a portion of the limited transmit power to the AN [5], [6], [10]. However, the secure RSMA designs of [5], [6], [10] considered the DL scenario, hence their results are not applicable to the UL due to the different nature of the problems. To the best of our knowledge, at the time of writing, no attention has been devoted to the integration of UL-RS with UAV-BS. Furthermore, the robust and secure design of RSMA-aided UAV networks relying on realistic imperfect CSI has not been investigated so far.

Given the knowledge gaps mentioned above, we consider a network in which the legitimate users aim for communicating with a UAV-BS in the presence of multiple passive *Eve*. In this UL scenario, each user employs RS, where the corresponding message of each user is split into two parts. Then, each user transmits a superposition of two messages having different power levels. To realize massive connectivity, we assume furthermore that at the network initialization a clustering process is accomplished by which the users are divided into different non-overlapping groups. Furthermore, due to the limited CSI feedback accuracy, a link outage may occur. Hence we introduce a maximum tolerable connection outage probability (COP) constraint for quantifying its impact on the system performance. It is worth mentioning that in contrast to the RSMA downlink in [5], [10], where the authors considered the secure design of the common streams, here we exploit a different strategy, where the transmission rate and the power allocated to each part of the bipartite messages is optimized in terms of *Effective Network Secrecy Throughput* (ENST) maximization. ENST is a secrecy performance metric quantifying the average secure throughput. More explicitly, when the reception reliability is considered to be similarly important to the security, then this parameter is considered. Mathematically, ENST is

formulated as the product of the target secrecy rate and the probability of successful reception as defined in [33, Eq. (5)]. Against this background, our contributions are summarized as follows:

- In addition to the COP constraint, which captures the impact of link outages, the secrecy outage probability (SOP) is tightly controlled to be under the tolerable level under unknown CSI of the *Eve*. We then maximize the ENST, subject to both COP and SOP constraints, as well as to the limited power budget. In particular, we design the RS power allocation at the users as well as the SIC-ordering corresponding to each cluster, so that the ENST is maximized.
- To deal with the resultant non-convex problem, we first derive a closed-form expression for characterizing the COP and a tight approximation of the SOP constraints. Then, we harness the two-tier block coordinate decent technique, where the optimization variables are estimated successively in an iterative manner. The first loop of this twin-tier approach maximizes the transmission rates, leading to a closed-form optimal solution relying on the Lambert W -function. By contrast, the second loop encounters some non-convexities, which are tackled by the powerful sequential parametric convex approximation (SPCA) method. The convex approximation of the non-convex factors are found with the aid of the first-order Taylor expansion.
- Our simulation results demonstrate that the proposed framework outperforms the existing non-orthogonal benchmarks in terms of the ENST criterion.

Our contributions are boldly and explicitly contrasted to the state-of-the-art at a glance in Table 1. The rest of this paper is organized as follows. The system model and channel definitions are provided in Section II. Section III describes the signal representation and formulates our ENST maximization problem. The proposed SPCA-based solution, the two-tier block coordinate decent procedures and our complexity analysis are provided in Section IV. In Section V, our simulation results are presented and the paper is concluded in Section VI. Finally, the Appendices and Proofs of the claims are provided in Section VII.

Notation: Vectors and matrices are denoted by

lower-case and upper-case boldface symbols, respectively; $(\cdot)^T$, $(\cdot)^*$, $(\cdot)^H$, and $(\cdot)^{-1}$ denote the transpose, conjugate, conjugate transpose, and inverse of a matrix respectively; $\Re(\cdot)$ denotes the real part of a complex variable, and $\Im(\cdot)$ the imaginary part of a complex variable; We use $\mathbb{E}\{\cdot\}$ and \triangleq to denote the expectation operation and a definition, respectively. A complex Gaussian random variable with mean μ and variance σ^2 reads as $\mathcal{CN}(\mu, \sigma^2)$, and $\text{Exp}(\lambda)$, $\text{Beta}(\alpha, \beta)$, and $\text{Gamma}(\gamma, \zeta)$ respectively denote the exponential distribution with mean λ , beta-distribution with parameters α and β , and gamma-distribution with shape γ and rate ζ . The principal branch of the Lambert W -function is defined by $W_0(x) e^{W_0(x)} = x$ for $x \geq -\frac{1}{e}$ with $W_0(x) \geq -1$ [19]; \mathbf{I}_N denotes the $N \times N$ identity matrix; $\mathbb{R}^{N \times 1}$ and $\mathbb{C}^{N \times 1}$ denote the set of N -dimensional standard real and complex Gaussian random variable, respectively; $\mathbb{C}^{N \times N}$ stands for an $N \times N$ element standard complex Gaussian random matrix whose real and imaginary parts are independent normally distributed random variables with a mean of zero and variance $\frac{1}{2}$. The notations $[x]^+$ and $\mathbb{P}(\cdot)$ stand for $\max\{x, 0\}$ and probability, respectively. The entry in the i -th row of a vector \mathbf{h} is represented by $\mathbf{h}[i]$. Furthermore, $\mathbf{u}^{max}\{\mathbf{A}\}$ and $\mathbf{v}^{max}\{\mathbf{A}\}$ denote the columns of \mathbf{U}_A and \mathbf{V}_A corresponding to the dominant singular value $\lambda^{max}\{\mathbf{A}\}$ of matrix \mathbf{A} , respectively, i.e., the matrix \mathbf{A} has a Singular Value Decomposition (SVD) given by $\mathbf{A} \triangleq \mathbf{U}_A \mathbf{\Lambda}_A \mathbf{V}_A$. Finally, $\angle(\mathbf{u}, \mathbf{v})$ represents the angle between vectors \mathbf{v} and \mathbf{u} .

II. SYSTEM MODEL

We consider the secure single-input multi-output (SIMO) uplink system, shown in Fig. 1. There are M clusters in the network considered, whose m^{th} cluster includes K_m number of single-antenna legitimate users gathered in the set $\mathcal{U}_m \triangleq \{U_{m,k}\}$, $\forall k \in \mathcal{K}_m \triangleq \{1, \dots, K_m\}$, who aim for transmitting to an N_t -antenna UAV-BS. We consider a massive access setting, where $\sum_{m=1}^M K_m \gg M$. Meanwhile, J number of non-cooperative passive N_e -antenna eavesdroppers (*Eves*) gathered in the set $\mathcal{E} \triangleq \{E_{e,j}\}$, $\forall j \in \mathcal{J} \triangleq \{1, \dots, J\}$, manage in covert wiretapping¹. Next, the channel models and

¹In this paper we have focused on non-colluding *Eve*'s who try to maximize their own SINR individually. The problem of colluding *Eves* has been left for future work.

TABLE I
BOLDLY AND EXPLICITLY CONTRASTING OUR CONTRIBUTIONS TO THE EXISTING LITERATURE.

References⇒ Keywords↓	Our Ap- proach	[1]	[2]	[3]	[4]	[5]	[6]	[7]	[8]	[9]	[10]	[11]	[12]	[13]	[14]	[15]	[16]	[17]	[18]
UAV-BS	✓	✓	✓	✓	✓	✓	✓												
UAV Trajectory Design		✓	✓																
IUI Management		✓	✓			✓	✓	✓											
IUI Cancellation	✓													✓					
SIC Ordering	✓													✓					
RSMA	✓			✓		✓	✓			✓	✓	✓	✓	✓					
NOMA									✓									✓	✓
SDMA								✓											
DL				✓		✓	✓		✓	✓	✓							✓	✓
UL	✓											✓	✓	✓				✓	
Limited Feedback Error	✓							✓	✓						✓				
Imperfect CSI	✓					✓	✓		✓		✓				✓			✓	
PLS	✓					✓	✓		✓		✓				✓	✓	✓	✓	✓
AN Design						✓										✓	✓		
Beamformer (precoder) Design	✓					✓	✓				✓					✓	✓	✓	✓
Power Allocation	✓					✓	✓		✓		✓					✓	✓	✓	
Known <i>Eve</i> with Imperfect E-CSIT						✓	✓				✓								✓
Worst-Case Secrecy Rate Maximization						✓	✓				✓								
Max-Min Fairness						✓	✓				✓	✓							
Sum-Rate Maximization									✓					✓					
Known <i>Eve</i>																			✓
Unknown <i>Eve</i>	✓															✓			
ICI Cancellation	✓																		
ENST Maximization	✓																		
COP Constraint	✓																		
SOP Constraint	✓																		

the clustering procedure operating under CSI error are described.

A. Channel Definitions

In our scenario, the $U_{m,k} \rightarrow E_{e,j}$ channels are represented by $\mathbf{q}_{m,j,k}$, $\forall m, k, j$, while the legitimate channels spanning from the terrestrial user to the UAV-BS, i.e., $U_{m,k} \rightarrow UAV$, are denoted by $\mathbf{h}_{m,k}$ $\forall m, k$. The ground-to-air (G2A) channels are modeled by $\mathbf{h}_{m,k} = \sqrt{PL(d_{m,k})} \mathbf{f}_{m,k}$, where $PL(d_{m,k}) \triangleq d_{m,k}^{-\alpha_{m,k}}$ represents the large-scale fading, while $d_{m,k}$ and $\mathbf{f}_{m,k} \sim \mathcal{CN}(0, \mathbf{I}_{N_i})$ therein, respectively, denote the G2A distance and

the corresponding small-scale fading. The path-loss exponent $\alpha_{m,k}$ obeys the probabilistic model [20], which is appropriate for low-altitude UAVs comprised of both the LoS and non-LoS components $\mathcal{L}_{m,k}$ and $\mathcal{N}_{m,k}$, given by:

$$\alpha_{m,k} \triangleq \frac{\mathcal{L}_{m,k} - \mathcal{N}_{m,k}}{1 + \lambda_1 \cdot \exp[\lambda_2 (\theta_{m,k} - \lambda_1)]} + \mathcal{N}_{m,k}, \quad (1)$$

where $\theta_{m,k}$ denotes the elevation angle between the UAV and user $U_{m,k}$, while λ_1 and λ_2 are the constants determined by the propagation environment [20].

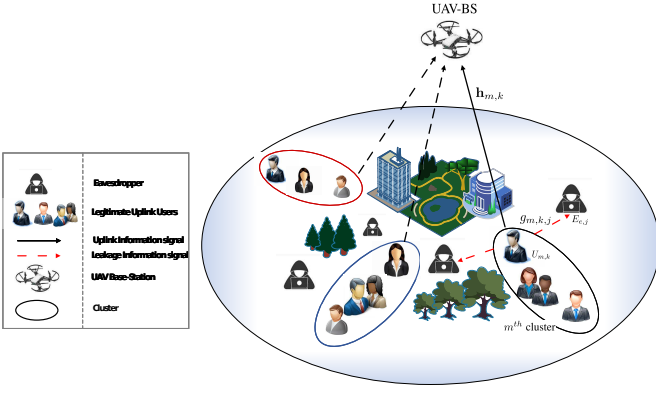


Fig. 1. The considered system model adopting RSMA

B. Clustering Under CSI Error

Given the slowly time-varying nature of the $PL(d_{m,k})$, we assume that both the UAV as well as the users can estimate it perfectly. However, due to the limited hardware complexity of the UAV, we assume that the UAV only captures the angle-of-arrival (AoA) information of the user-UAV channel, and even this AoA information is imperfect. To elaborate a little further, first the UAV broadcasts a sequence of training symbols towards the ground users, who aim for acquiring the knowledge of their own DL channels. In general, given a sufficiently high transmit power, as well as a long training sequence, legitimate users are capable of perfectly estimating their own channels. More explicitly, all the users within the m^{th} cluster have the same AoA and thus we can construct a codebook \mathcal{V} , comprised of M unit-norm vectors $\{\mathbf{v}_m\}_{m=1}^M \in \mathbb{C}^{N_t \times 1}$. At the network's initialization, this codebook is randomly generated and made known off-line to both the UAV and the users for example via the codebook distribution regime of [22]. To convey the corresponding AoA to the UAV, each $U_{m,k}$ quantizes its channel direction, i.e., $\tilde{\mathbf{f}}_{m,k} \triangleq \frac{\mathbf{f}_{m,k}}{\|\mathbf{f}_{m,k}\|}$, to the closest vector in terms of the chordal distance metric of ² [23], [24]:

$$\hat{\mathbf{f}}_{m,k} \triangleq \arg \max_{\mathbf{v}_m \in \mathcal{V}} \left| \tilde{\mathbf{f}}_{m,k}^H \mathbf{v}_m \right|^2 = \arg \max_{\mathbf{v}_m \in \mathcal{V}} \cos^2 \left[\angle \left(\tilde{\mathbf{f}}_{m,k}, \mathbf{v}_m \right) \right]. \quad (2)$$

Accordingly, the users having the maximum chordal distance between their so-obtained channel direction $\tilde{\mathbf{f}}_{m,k}$ and \mathbf{v}_m are allocated to the m^{th} cluster and the number of users within each cluster, i.e., K_m , is also updated after the grouping. Now, each user sends

²The optimal vector quantization strategy in multi-user uplink channels, even in single-cell systems, is not known in general and is beyond the scope of our work.

the corresponding codebook index back to the UAV using $B \triangleq \lceil \log_2 M \rceil$ bits through an error-free and delay-free feedback channel. However, because of the limited feedback per channel coherence block as well as the instability of the UAV platform, the CSI of the main channel obtained at the UAV is imperfect. Thus, a quantization error in the form of

$$\tilde{\mathbf{f}}_{m,k} = \cos(\phi_{m,k}) \hat{\mathbf{f}}_{m,k} + \sin(\phi_{m,k}) \mathbf{e}_{m,k}, \quad (3)$$

appears in the AoA estimates of users, where $\mathbf{e}_{m,k} \in \mathbb{C}^{N_t \times 1}$ is the unit-norm quantization error vector isotropically distributed in the null-space of $\tilde{\mathbf{f}}_{m,k}$, while $\phi_{m,k} \triangleq \angle \left(\tilde{\mathbf{f}}_{m,k}, \mathbf{v}_m \right)$ of (3) represents the angle between $\tilde{\mathbf{f}}_{m,k}$ and \mathbf{v}_m , and $\sin^2(\phi_{m,k})$ being a random variable, whose variance is determined by B [25]. To visualize the proposed approach, the whole procedure is shown in Fig. 2, while further details will be presented in the sequel.

III. SIGNAL REPRESENTATION AND PROBLEM FORMULATION

In the RSMA uplink, each $U_{m,k}$ within the m^{th} cluster transmits a superposition code of two normalized sub-messages $s_{m,k,n}|_{n=1}^2$, i.e., $\mathbb{E} \{|s_{m,k,n}|^2\} = 1$, given by [26]:

$$s_{m,k} = \sum_{n=1}^2 \sqrt{p_{m,k,n}} s_{m,k,n}, \quad \forall k \in \mathcal{K}_m, \quad (4)$$

where $p_{m,k,n}$, $\forall n \in \{1, 2\}$ corresponds to the transmit power of $s_{m,k,n}$ $\forall n \in \{1, 2\}$. During the uplink signal reception, the UAV relies on beamforming for discriminating the signals received by suppressing the IUI. Therefore, as shown in Fig. 3, the signal received at the UAV, i.e., y_{UAV} , is passed through M different angularly selective filters $\{\mathbf{w}_m\}_{m=1}^M \in \mathbb{C}^{N_t \times 1}$, distributed in M branches. Accordingly, the m^{th} signal (i.e., the m^{th} branch) received by the UAV and the received signal at *Eves*, respectively denoted by $y_{\text{UAV},m}$ and $y_{e,j}$, are formulated as follows:

$$y_{\text{UAV}} = \sum_{i=1}^M \left(\sum_{k=1}^{K_i} \mathbf{h}_{i,k} s_{i,k} \right) + \mathbf{z}, \quad (5)$$

$$y_{\text{UAV},m} = \mathbf{w}_m^H (y_{\text{UAV}}),$$

$$y_{e,j} = \mathbf{w}_{m,j}^H (\mathbf{Q}_{m,j} \mathbf{s}_m + \mathbf{z}_{m,j}), \quad \forall j \in \mathcal{J}, \quad (6)$$

where $\mathbf{Q}_{m,j} \triangleq [\mathbf{q}_{m,j,1}, \mathbf{q}_{m,j,2}, \dots, \mathbf{q}_{m,j,K}]$, $\mathbf{s}_m \triangleq [s_{m,1}, s_{m,2}, \dots, s_{m,K}]^T$, $\mathbf{z}_m \triangleq \mathbf{w}_m^H \mathbf{z}_m \sim \mathcal{CN}(0, \sigma_m^2)$

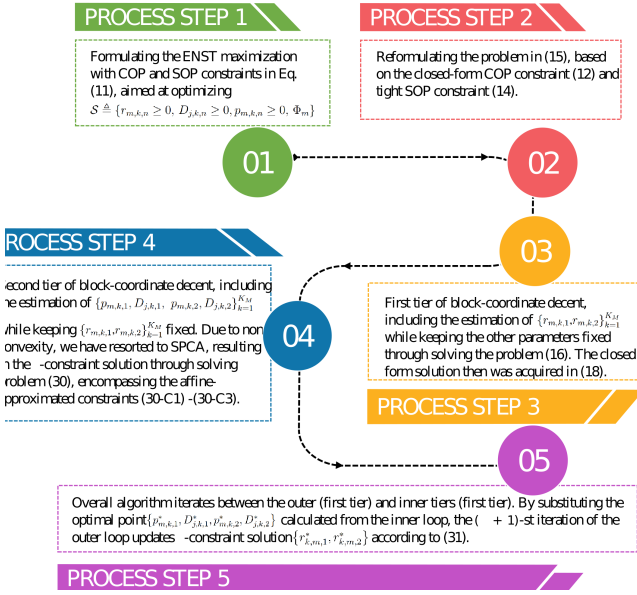


Fig. 2. The algorithmic procedure of the proposed method

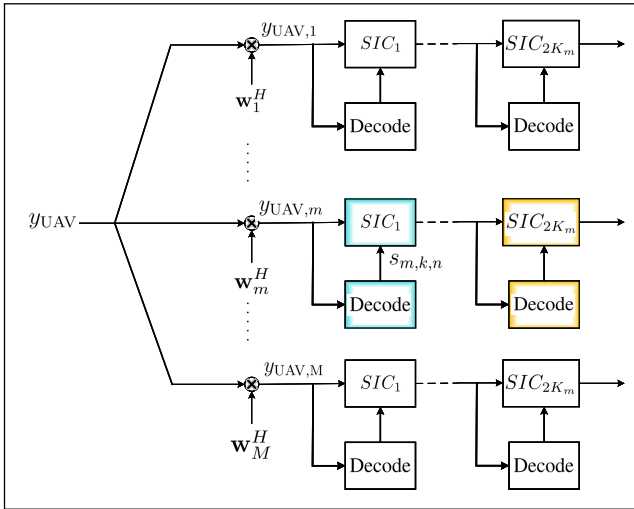


Fig. 3. RSMA-based BS structure in M -Cluster UL communications.

and $\mathbf{z}_{m,j} \sim \mathcal{CN}(0, \sigma_e^2 \mathbf{I}_{N_e})$ represent the additive white Gaussian noise (AWGN) due to the m^{th} cluster at the UAV and at the j^{th} *Eve*, respectively. $\mathbf{w}_{m,j} \triangleq \mathbf{u}^{\max} \{\tilde{\mathbf{Q}}_{m,j}\}$ represents the MRC beamformer employed by *Eve* where $\tilde{\mathbf{Q}}_{m,j} \triangleq \mathbf{Q}_{m,j} (\mathbf{Q}_{m,j})^H$. It is easy to show that $y_{e,j} = \sum_{k=1}^{K_m} g_{m,k,j} s_{m,k} + \xi_{e,j}, \forall j \in \mathcal{J}$, where

$$g_{m,k,j} \sim \mathcal{CN}\left(0, \sqrt{\lambda_j^{\max} \{\tilde{\mathbf{Q}}_{m,j}\}}\right) [21], \text{ and } \xi_{e,j} \sim \mathcal{CN}(0, \sigma_e^2). \text{ In terms of the worst-case secrecy}$$

scenario, *Eve* is assumed to be able to perfectly estimate its corresponding CSI and no ICI is available to degrade the performance of *Eve*. To force the ICI terms to zero, we resort the zero-forcing (ZF) beamforming. More explicitly, upon relying on the codebook \mathcal{V} discussed earlier in Section I.B, \mathbf{w}_m is chosen so that we have $\mathbf{w}_m^H \mathbf{v}_l = 0, \forall l \neq m, l \in \{1, 2, \dots, M\}$.

when considering the signal extracted from the m^{th} cluster, the UAV employs $2K_m$ number of SIC stages to suppress IUI as well as to decode all transmitted messages in the set $\mathcal{K}_{m,n} \triangleq \{s_{m,k,n}\}$ received from $y_{\text{UAV},m}$, as illustrated in Fig. 3. The decoding order of the m^{th} cluster at the UAV is denoted by a permutation Φ_m , which belongs to set Π_m defined as the set of all possible decoding orders of all $2K_m$ messages arriving from K_m users, which includes $\frac{2K_m!}{2^{K_m}}$ elements. Let $\Phi_{m,k,n}$ represents the position of the message $s_{m,k,n}$ in Φ_m . Therefore, we can define $\Phi_{m,k,n} = \{(k', n') \neq (k, n) \mid (k', n') \succ (k, n)\}$, where the operator $(k', n') \succ (k, n)$ indicates that $s_{m,k,n}$ has a higher decoding order than $s_{m,k',n'}$ in Φ_m , i.e., the UAV is scheduled to decode $s_{m,k',n'}$ after decoding and cancelling out the effect of $s_{m,k,n}$.

Therefore, in the SIC scheme of the RSMA uplink, the UAV first decodes and subtracts the remodulated signals having higher decoding orders. i.e., $(k', n') \in \mathcal{K}_{m,n} \setminus \{(k, n) \cup \Phi_{m,k,n}\}$, then it decodes signal $s_{m,k,n}$, where the signal of the users in $\Phi_{m,k,n}$ is treated as noise. According to the SIC protocol, the signal of $s_{m,k,n}$ will be decoded prior to $s_{m,k',n'}$ if we have $|\Phi_{m,k,n}| > |\Phi_{m,k',n'}|$, where $|\mathcal{A}|$ is the cardinality of the set \mathcal{A} . Accordingly, the signal-to-interference-plus-noise ratio (SINR) at the UAV experienced upon detecting $s_{m,k,n}$, and denoted by $\rho_{m,k,n}$ is formulated as (7), where the IUI and ICI terms are obtained by substituting (4) into (7). Notably, after clustering in the presence of beamforming weight quantization errors the ICI cannot be completely removed by the beamformer having the weights of \mathbf{w}_m , thus a residual ICI term contaminates the corresponding received signal of the m^{th} cluster. In other words, the beamformer weights \mathbf{w}_m fail to perfectly null out the ICI due to the limited feedback.

Furthermore, it is assumed that the *Eves* have no information about Φ_m , hence they cannot perform

$$\begin{aligned}
\rho_{m,k,n} &= \frac{p_{m,k,n} |\mathbf{w}_m^H \mathbf{h}_{m,k}|^2}{\sum_{(k',n') \in \Phi_{m,k,n}} p_{m,k',n'} |\mathbf{w}_m^H \mathbf{h}_{m,k'}|^2 + \sum_{i=1, i \neq m}^M \sum_{k''=1}^{K_i} P_{i,k''} |\mathbf{w}_m^H \mathbf{h}_{i,k''}|^2 + \sigma_m^2} \quad (7) \\
&= \frac{p_{m,k,n} \text{PL}(d_{m,k}) |\mathbf{w}_m^H \mathbf{f}_{m,k}|^2}{\underbrace{\sum_{(k',n') \in \Phi_{m,k,n}} p_{m,k',n'} \text{PL}(d_{m,k'}) |\mathbf{w}_m^H \mathbf{f}_{m,k'}|^2}_{\text{IUI}} + \underbrace{\sum_{i=1, i \neq m}^M \sum_{k''=1}^{K_i} P_{i,k''} \text{PL}(d_{i,k''}) \|\sin(\phi_{i,k''}) \mathbf{f}_{i,k''}\|^2 |\mathbf{w}_m^H \mathbf{e}_{i,k''}|^2}_{\text{ICI}} + \sigma_m^2}
\end{aligned}$$

SIC within a cluster³. Consequently, from the perspective of $E_{e,j}$, the received SINR of decoding $s_{m,k,n}$, while treating the other ones as noise, is formulated as:

$$\mu_{j,k,n} = \frac{p_{m,k,n} \text{PL}(d_{m,k,j}) |g_{m,k,j}|^2}{\sum_{(k',n') \neq (k,n)} p_{m,k',n'} \text{PL}(d_{m,k',j}) |g_{m,k',j}|^2 + \sigma_e^2}. \quad (8)$$

Given the SINRs in (7) and (8), the corresponding achievable rates are respectively given by $C_{m,k,n} \triangleq \log_2(1 + \rho_{m,k,n})$ and $C_{j,k,n} \triangleq \log_2(1 + \mu_{j,m,n})$.

Remark 1. For ensuring reliable uplink communication, the transmission rate $r_{m,k,n}$ of each $U_{m,k}$ should not exceed $C_{m,k,n}$, i.e., $C_{m,k,n} \geq r_{m,k,n}$. However, as a consequence of ICI and fading, $r_{m,k,n}$ might violate this condition, hence leading to the link outages. However, the COP, defined as the probability that a system is unable to support the target transmission rate $C_{m,k,n}$, must be limited by the maximum tolerable COP $\epsilon_{cop} \in (0, 1)$, as follows:

$$\text{COP} : P_{m,k,n}^{CO} \triangleq \mathbb{P}\{r_{m,k,n} > C_{m,k,n}\} \leq \epsilon_{cop}. \quad (9)$$

Remark 2. On the other hand, since the $U_{m,k}$ has no knowledge concerning the CSIs of passive *Eves* [28], the values of $\mu_{j,m,n}$ are unknown. A beneficial secrecy policy in this situation is to adjust the redundancy rate of $U_{m,k}$ [28], denoted by $D_{j,k,n}$, so that the COP limit of (9) is satisfied. In other words, $D_{j,k,n}$ must not exceed $C_{j,k,n}$. To do so, the

SOP of $\epsilon_{sop} \in (0, 1)$, satisfies:⁴

$$\text{SOP} : P_{j,k,n}^{SO} \triangleq \mathbb{P}\{D_{j,k,n} \leq C_{j,k,n}\} \leq \epsilon_{sop}. \quad (10)$$

Remark 3. Upon considering non-colluding *Eves*, the achievable secrecy rates of $U_{m,k}$ where transmitting $s_{k,m,n}$ is limited by the worst-case *Eve* scenario of $C_{m,k,n}^{sec} \triangleq \min_{1 \leq j \leq J} \{[r_{m,k,n} - D_{j,k,n}]^+\}$. On

the other hand, while minimizing $P_{m,k,n}^{CO}$ would improve the reliability, maximizing $C_{m,k,n}^{sec}$ will enhance the security upon jointly considering both the reliability and security requirements of all $U_{m,k}|_{k=1}^{K_m}$, we should rather maximize the ENST, defined as $C_{ENST} \triangleq \sum_{k=1}^{K_m} \sum_{n=1}^2 (1 - P_{m,k,n}^{CO}) C_{m,k,n}^{sec}$.

Based on the discussion in Remarks 1-3, while considering the limited power budget imposed on each $U_{m,k}$, formulated as $\sum_{n=1}^2 p_{m,k,n} \leq P_{m,k}$, the optimization problem of the proposed secure RSMA-based uplink is formulated as:

$$\max_{\mathcal{S}} \left(\min_{1 \leq j \leq J} \left\{ \sum_{k=1}^{K_m} \sum_{n=1}^2 (1 - P_{m,k,n}^{CO}) [r_{m,k,n} - D_{j,k,n}]^+ \right\} \right) \quad (11)$$

s.t.

$$C_1 : P_{m,k,n}^{CO} \leq \epsilon_{cop}, \quad \forall k,$$

$$C_2 : P_{j,k,n}^{SO} \leq \epsilon_{sop}, \quad \forall k, j,$$

$$C_3 : \sum_{n=1}^2 p_{m,k,n} \leq P_{m,k}, \quad p_{m,k,n} \geq 0, \quad \forall k,$$

where $\mathcal{S} \triangleq \{r_{m,k,n} \geq 0, D_{j,k,n} \geq 0, p_{m,k,n} \geq 0, \Phi_m\}$.

⁴It should be highlighted that, we considered the worst-case condition for ensuring both reliability and security of each part of split messages. This implies that if actual transmission rate of each split messages $s_{m,k,n} \forall n \in \{1, 2\}$ corresponding to $U_{m,k}$ can satisfy its target transmission rate $C_{m,k,n} \forall n \in \{1, 2\}$, as stipulated in the COP condition of (9), we can guarantee that the per user basis condition is also met. At the receiver, UAV-BS recover and merges each of these two split messages corresponding to each user separately to retrieve their original messages. Thus, the conditions described above, should be satisfied for each part of message separately. We can use the same justification for the SOP constraint (10).

³As a more challenging secrecy scenario, for comparison, in our simulation we consider a scenario when $E_{e,j}$ can exploit the optimal SIC decoding order and receives no CSI.

Due to the non-convex OF, as well as the discontinuous variable Φ_m , the problem in (11) represents a non-convex mixed integer programming problem. In the next section, we derive closed-form expressions both for the COP and SOP constraints, while Φ_m is obtained through an exhaustive search.

IV. ENST MAXIMIZATION SOLUTION

In this section, we construct the overall algorithm for finding the optimal solution of (11).

A. Handling the Probabilistic Constraints (11)- C_1 and (11)- C_2

We first intend to handle the COP constraint (11)- C_1 . In this regard, we first insert (7) into (9), so that (11)- C_1 may be reformulated as (12), where we have $\beta_{m,n,k} = 2^{r_{m,k,n}} - 1$, $\lambda_{m,k',n'} \triangleq \frac{1}{2p_{m,k',n'} \text{PL}(d_{m,k'})}$, and $\lambda_{i,k''} = \frac{2^{\frac{B}{N_t-1}}}{P_{i,k''} \text{PL}(d_{i,k''})}$ (*Proof*: See Appendix A).

Upon inserting (8) into (10), we may reformulate the SOP constraint (11)- C_2 as (13), where we have $\eta_{j,k,n} = \frac{1}{p_{m,k,n} \text{PL}(d_{m,k,j}) \lambda_j^{\max} \{\mathcal{Q}_{m,j}\}}$, $\zeta_{j,k',n'} = \frac{1}{p_{m,k',n'} \text{PL}(d_{m,k',j}) \lambda_j^{\max} \{\mathcal{Q}_{m,j}\}}$, and $\kappa_{j,k,n} = 2^{D_{j,k,n}} - 1$ (*Proof*: See Appendix B). On the other hand, since $D_{j,k,n}$ independent of both $r_{k,m,n}$ and $p_{k,m,n}$ within the OF, the maximization problem (11) over $D_{j,k,n}$ is equivalent to minimizing $D_{j,k,n}$. To find a more conservative solution, we exploit that $D_{j,k,n}$ appears both in the OF and in the SOP constraint (11), we have to exploit a tighter constraint than (13) for obtaining the minimum value of $D_{j,k,n}$, which is given by (14), where $W_0(x)$ is the Lambert W -function (*Proof*: See Appendix C). However, it is still challenging to solve (11), since $r_{k,m,n}$ and $p_{k,m,n}$ are coupled in the OF of (11). To arrive at a more tractable form, the operations of maximization and the minimization can be swapped in (11). Additionally, since $\{D_{j,k,n}\}_{j=1}^M$ are independent, we can actually solve J independent maximization problems and then simply choose the minimum one. Furthermore, by exploiting the inequalities of $\exp(-x) \leq \frac{1}{1+x}$ and $\frac{1}{1+x} \leq \frac{1}{x}$, we can instead replace the lower bound and upper bound of the OF and of the COP constraint (11), respectively. Accordingly, based on what was mentioned above, a bound of the solution may be obtained as (15), where we have $A \triangleq |\Phi_{m,k,n}| + M + K_i$, $\xi \triangleq \prod_{i=1, i \neq m}^M \prod_{k''=1}^{K_i} 2\lambda_{i,k''}^{-1}$.

Now, we can exploit the block coordinate decent technique, where $\{p_{m,k,1}, D_{j,k,1}, p_{m,k,2}, D_{j,k,2}\}_{k=1}^{K_M}$ and the $\{r_{m,k,1}, r_{m,k,2}\}_{k=1}^{K_M}$ are found successively in an iterative manner. In particular, the l^{th} iteration of the algorithm is constituted by separately maximizing the criterion with respect to each of $\{r_{m,k,1}, r_{m,k,2}\}_{k=1}^{K_M}$ and $\{p_{m,k,1}, D_{j,k,1}, p_{m,k,2}, D_{j,k,2}\}_{k=1}^{K_M}$, while keeping the other one fixed. Given this perspective, we first update $\{r_{m,k,1}, r_{m,k,2}\}_{k=1}^{K_M}$, while assuming that $\{p_{m,k,1}, D_{j,k,1}, p_{m,k,2}, D_{j,k,2}\}_{k=1}^{K_M}$ are fixed values which results in the following optimization problem:

$$\min_{1 \leq j \leq J} \left(\max_{\{r_{m,k,1}, r_{m,k,2}\}} \left\{ \sum_{k=1}^{K_M} \sum_{n=1}^2 \exp \left(\Xi_{m,n}^r \frac{\beta_{m,n,k}}{2} \right) r_{m,k,n} \right\} \right), \quad (16)$$

s.t.

$$\xi \exp \left(-\frac{\beta_{m,n,k} \sigma_m^2}{2} \right) \beta_{m,n,k}^{-A} \prod_{(k',n') \in \Phi_{m,k,n}} \left(2\lambda_{m,k',n'}^{*-1} \right) \leq \epsilon_{cop},$$

$$\forall k, n, \text{ where } \Xi_{m,n}^r \triangleq \sum_{(k',n') \in \Phi_{m,k,n}} \lambda_{m,k',n'}^{*-1} + \xi - \sigma_m^2.$$

It is easy to check that in terms of $\{r_{m,k,1}, r_{m,k,2}\}_{k=1}^{K_M}$, while the OF of (16) is an increasing function, while constraint (16)- C_1 is a decreasing one. Hence, the closed form expression of $\{r_{m,k,1}, r_{m,k,2}\}_{k=1}^{K_M}$ may be obtained when the inequality constraint (16)- C_1 is active at the optimum. Hence, the optimal point of (16), i.e., $\{r_{m,k,1}^*, r_{m,k,2}^*\}_{k=1}^{K_M}$, may be found by solving the following equation:

$$\exp \left(-\frac{\sigma_m^2 \beta_{m,n,k}}{2} \right) \beta_{m,n,k}^{-A} = \frac{\epsilon_{cop}}{\xi} \prod_{(k',n') \in \Phi_{m,k,n}} \left(\frac{\lambda_{m,k',n'}^*}{2} \right). \quad (17)$$

By doing so, followed by some algebraic manipulations, together with the help of the principal branch of the Lambert W -function, the optimum is formulated as follows:

$$r_{m,k,n}^* = \log_2 \left(1 + \frac{2A}{\sigma_m^2} W_0 \left(\left[\xi \epsilon_{cop}^{-1} \prod_{(k',n') \in \Phi_{m,k,n}} \left(2\lambda_{m,k',n'}^{*-1} \right) \right]^{\frac{1}{A}} \right) \right). \quad (18)$$

Now, assuming $\{r_{m,k,1}^*, r_{m,k,2}^*\}_{k=1}^{K_M}$ to be fixed values, we can update $\{p_{m,k,1}, D_{j,k,1}, p_{m,k,2}, D_{j,k,2}\}_{k=1}^{K_M}$, which result in the following equivalent transformation of (16) in the log-domain as (19), where $\mathcal{F}_j \triangleq \sum_{k=1}^{K_M} \sum_{n=1}^2 \beta_{m,n,k}^*$

$$\gamma \triangleq \frac{\sum_{(k',n') \in \Phi_{m,k,n}} \text{PL}(d_{m,k'}) p_{m,k',n'} + \ln [r_{m,k,n}^* - D_{j,k,n}]}{2^{-2} |\Phi_{m,k,n}| \epsilon_{cop} \xi^{-1} \exp \left(\frac{\beta_{m,n,k}^* \sigma_m^2}{2} \right)},$$

$$P_{m,k,n}^{CO} \triangleq \mathbb{P} \{r_{m,k,n} > \log_2(1 + \rho_{m,k,n})\} \quad (12)$$

$$= 1 - \exp\left(-\frac{\beta_{m,n,k}\sigma_m^2}{2}\right) \prod_{(k',n') \in \Phi_{m,k,n}} \left(1 + \lambda_{m,k',n'}^{-1} \frac{\beta_{m,n,k}}{2}\right)^{-1} \prod_{i=1}^M \prod_{i \neq m, k''=1}^{K_i} \left(1 + \lambda_{i,k''}^{-1} \frac{\beta_{m,n,k}}{2}\right)^{-1}, \forall k \in \mathcal{K}_m$$

$$P_{j,k,n}^{SO} \triangleq \mathbb{P} \{D_{j,k,n} \leq \log_2(1 + \mu_{j,k,n})\} = \exp(-\eta_{j,k,n} \kappa_{j,k,n} \sigma_e^2) \prod_{(k',n') \neq (k,n)} \left(1 + \eta_{j,k,n} \kappa_{j,k,n} \zeta_{j,k',n'}^{-1}\right)^{-1}, \quad (13)$$

$$D_{j,k,n} \leq \log_2 \left(1 + \frac{2K_m - 1}{\eta_{j,k,n} \sigma_e^2} W_0 \left(\frac{\eta_{j,k,n} \sigma_e^2}{2K_m - 1} \left(\frac{\prod_{(k',n') \neq (k,n)} \zeta_{j,k',n'}}{\eta_{j,k,n}} \epsilon_{sop}^{-1} \right)^{\frac{1}{2K_m - 1}} \right) \right), \quad (14)$$

$$\min_{1 \leq j \leq J} \left(\max_S \left\{ \sum_{k=1}^{K_m} \sum_{n=1}^2 \exp\left(\frac{\beta_{m,n,k}}{2} \left[\sum_{(k',n') \in \Phi_{m,k,n}} \lambda_{m,k',n'}^{-1} + \xi - \sigma_m^2 \right] \right) [r_{m,k,n} - D_{j,k,n}]^+ \right\} \right) \quad (15)$$

s.t.

$$C_1 : \xi \exp\left(-\frac{\beta_{m,n,k}\sigma_m^2}{2}\right) \beta_{m,n,k}^{-A} \prod_{(k',n') \in \Phi_{m,k,n}} 2\lambda_{m,k',n'}^{-1} \leq \epsilon_{cop}, \quad \forall k, n$$

$$C_2 : D_{j,k,n} \leq \log_2 \left(1 + \frac{2K_m - 1}{\eta_{j,k,n} \sigma_e^2} W_0 \left(\frac{\eta_{j,k,n} \sigma_e^2}{2K_m - 1} \left(\frac{\prod_{(k',n') \neq (k,n)} \zeta_{j,k',n'}}{\eta_{j,k,n}} \epsilon_{sop}^{-1} \right)^{\frac{1}{2K_m - 1}} \right) \right), \quad \forall k, j, n$$

$$C_3 : \sum_{n=1}^2 p_{m,k,n} \leq P_{m,k}, \quad p_{m,k,n} \geq 0, \quad \forall k,$$

$\beta_{m,n,k}^{(|\Phi_{m,k,n}| + M + K_i)}$, and $\psi_k \triangleq \log_2(\gamma) - \sum_{(k',n') \in \Phi_{m,k,n}}$
 $\log_2(\text{PL}(d_{m,k'}))$.

Note that the newly added constraint (19)- C_3 arises from the fact that the point-wise maximum operator $[\cdot]^+$ within the OF of (15) leads to non-convexity. Thus, by adding (19)- C_3 we are equivalently stating that the OF must be non-negative at the optimum and then we can simply remove $[\cdot]^+$. Now, since the OF in (19) is constituted by the sum of convex and affine functions with respect to $\{p_{m,k,1}, D_{j,k,1}, p_{m,k,2}, D_{j,k,2}\}_{k=1}^{K_M}$, it is a convex function. However, problem (19) is still non-convex because of the non-convex constraint (19)- C_2 . To circumvent the non-convexity, we harness the SPCA of [5], [15], where the non-convex factor is approx-

imated by its first-order Taylor expansion at each iteration. Given this perspective, in the following we attempt to circumvent the non-convexity imposed by the fractional form and the logarithmic function within (19)- C_2 by introducing some auxiliary variables, namely $\{\theta_{j,k,n}, \varrho_{j,k,n}, \nu_{j,k,n}, \vartheta_{j,k,n}\}$. Following the classic variable transformation approach, the constraint (19)- C_2 can be decomposed into $\forall k, j, n$:

$$D_{j,k,n} \leq \log_2(1 + \theta_{j,k,n}), \quad \forall k, j, n, \quad (20)$$

$$\theta_{j,k,n} \geq \frac{\text{PL}(d_{m,k,j})(2K_m - 1)}{\sigma_e^2} p_{m,k,n} \varrho_{j,k,n}, \quad (21)$$

$$\varrho_{j,k,n} \geq W_0(\nu_{j,k,n}), \quad (22)$$

$$\nu_{j,k,n} p_{m,k,n}^{2K_m} \geq \frac{\sigma_e^2}{\text{PL}(d_{m,k,j})^{2K_m} (2K_m - 1)} \vartheta_{j,k,n}, \quad (23)$$

$$\min_{1 \leq j \leq J} \left(\max_{\{p_{m,k,1}, D_{j,k,1}, p_{m,k,2}, D_{j,k,2}\}_{k=1}^{K_M}} \{\mathcal{F}_j\} \right), \quad (19)$$

s.t.

$$C_1 : \sum_{(k',n') \in \Phi_{m,k,n}} \log_2(p_{m,k',n'}) \leq \psi_k, \quad C_3 : r_{m,k,n}^* \geq D_{j,k,n}, \quad C_4 : \sum_{n=1}^2 p_{m,k,n} \leq P_{m,k}, p_{m,k,n} \geq 0,$$

$$C_2 : D_{j,k,n} \leq \log_2 \left(1 + \frac{2K_m - 1}{\eta_{j,k,n} \sigma_e^2} W_0 \left(\frac{\prod_{(k',n') \neq (k,n)} \zeta_{j,k',n'}}{\eta_{j,k,n}} \epsilon_{sop}^{-1} \right)^{\frac{1}{2K_m - 1}} \right), \quad \forall k, j, n$$

$$\vartheta_{j,k,n} \geq \left(\prod_{(k',n') \neq (k,n)} \zeta_{j,k',n'} \epsilon_{sop}^{-1} \right)^{\frac{1}{2K_m - 1}}. \quad (24)$$

Now, since the non-convexity still persists within (20)-(24), we attempt to approximate the non-convex factor at each iteration by its first-order Taylor expansion at the t^{st} SPCA iteration. Following this approach, the affine approximation becomes straightforward for each of (20)-(24). Hence, we can replace each non-convex constraint by its affine approximation, and thus the equivalent convex form of (19)- C_2 at the t^{st} SPCA iteration may be formulated as:

$$2^{D_{j,k,n}} \leq 1 + \theta_{j,k,n}, \quad (25)$$

$$\theta_{j,k,n} \geq \frac{\text{PL}(d_{m,k,j})(2K_m - 1)}{\sigma_e^2} \Theta^{[t]}(p_{m,k,n}, \varrho_{j,k,n}), \quad (26)$$

$$\varrho_{j,k,n} \geq W_0(\nu_{j,k,n}^{[t]}) \left(\nu_{j,k,n}^{[t]} (1 - W_0(\nu_{j,k,n}^{[t]})) \right)^{-1} (\nu_{j,k,n} - \nu_{j,k,n}^{[t]}), \quad (27)$$

$$\Psi^{[t]}(\nu_{j,k,n}, p_{m,k,n}^{2K_m}) \geq \frac{\sigma_e^2}{\text{PL}(d_{m,k,j})^{2K_m} (2K_m - 1)} \vartheta_{j,k,n}, \quad (28)$$

$$\log(\vartheta_{j,k,n}) \geq \frac{1}{(2K_m - 1)} \left(\sum_{(k',n') \neq (k,n)} \Lambda^{[t]}(\zeta_{j,k',n'}) - \log(\epsilon_{sop}) \right) \quad (29)$$

$$\begin{aligned} \forall k, j, n, \quad \text{respectively,} \quad \Theta^{[t]}(p_{m,k,n}, \varrho_{j,k,n}) &\triangleq \frac{1}{4}(p_{m,k,n} + \varrho_{j,k,n})^2 + \frac{1}{4}(p_{m,k,n} - \varrho_{j,k,n})^2 - \frac{1}{2}(p_{m,k,n} - \varrho_{j,k,n}) \\ &(p_{m,k,n} - \varrho_{j,k,n}), \quad \Gamma^{[m]}(D_{j,k,n}) \triangleq 2^{D_{j,k,n}} \\ &\left[1 + \ln(2) \left(D_{j,k,n} - D_{j,k,n}^{[t]} \right) \right], \quad \Lambda^{[t]}(\zeta_{j,k',n'}) \triangleq \log(\zeta_{j,k',n'}^{[t]}) \\ &+ \frac{\zeta_{j,k',n'} - \zeta_{j,k',n'}^{[t]}}{\zeta_{j,k',n'}^{[t]}}, \quad \text{and} \quad \Psi^{[t]}(\nu_{j,k,n}, p_{m,k,n}^{2K_m}) \triangleq \nu_{j,k,n} \\ &\left(p_{m,k,n}^{[t]} \right)^{2K_m} + \left(p_{m,k,n} \right)^{(2K_m - 1)} \left[\left(p_{m,k,n}^{[t]} \right)^T \right. \\ &\left. \nu_{j,k,n}^{[t]} \right] \times \left[\nu_{j,k,n} - \nu_{j,k,n}^{[t]}, p_{m,k,n} - p_{m,k,n}^{[t]} \right]. \end{aligned}$$

In order to arrive at (27) from (22), we have exploited the fact that since $W_0(x)$ is concave over the interval of $(-e^{-1}, \infty)$ and positive over $(1, \infty)$, upon using the first order Taylor expansion of $W_0(x)$ we have $W_0(\nu_{j,k,n}) \leq W_0(\nu_{j,k,n}^{[t]}) \left[\nu_{j,k,n}^{[t]} \right.$

$$\left. \left(1 - W_0(\nu_{j,k,n}^{[t]}) \right) \right]^{-1} (\nu_{j,k,n} - \nu_{j,k,n}^{[t]}).$$

B. Overall Solution of the Original Problem (11)

Note that due to the decoding order constraint $\{\Phi_m\}$, it is challenging to find the optimal solution of problem (11). To solve this problem, we first fix the decoding order Φ_m to obtain the optimal triplet $\{r_{k,m,n}^* \geq 0, D_{j,k,n}^* \geq 0, p_{m,k,n}^* \geq 0\}$ and then exhaustively search the entire set to find the optimal Φ_m^* ⁵. Upon assuming a fixed Φ_m , we conceive a two-tier iterative algorithm for attaining the overall ϵ -constraint solution $\{p_{m,k,1}^*, D_{j,k,1}^*, p_{m,k,2}^*, D_{j,k,2}^*\}$ in two different tiers. More explicitly, using the approximations obtained in (25)-(29), together with $\{r_{k,m,1}^*, r_{k,m,2}^*\}$ gleaned from the outer tier, the $(t+1)^{st}$ iteration of the inner tier solves the following equivalent convex form of problem (19) for finding the ϵ -constraint solution as (30), where $\mathbf{X} \triangleq (\mathbf{x}, \{p_{m,k,1}, D_{j,k,1}, p_{m,k,2}, D_{j,k,2}\}_{k=1}^{K_M})$, and $\mathbf{x} \triangleq \{\theta_{j,k,n}, \varrho_{j,k,n}, \nu_{j,k,n}, \vartheta_{j,k,n}, \nu_{j,k,n}\}$. Upon the ϵ -constraint point $\{p_{m,k,1}^*, D_{j,k,1}^*, p_{m,k,2}^*, D_{j,k,2}^*\}$ found by the inner loop, the $(q+1)^{st}$ iteration of the outer loop finds ϵ -constraint solution $\{r_{m,k,1}^{*[q+1]}, r_{m,k,2}^{*[q+1]}\}$, given by (31), where the superscript “*” represents the final iteration of the inner loop. Since the proposed method consists of two layers of iterations, the stopping criterion of each layer depends on the relative change of the two consecutive of values. Therefore, the outer loop proceeds to the next iteration

⁵Although it would also be beneficial to look for an optimal SIC-ordering [5], [6], as the UAV is assumed to only have access to the AoA and distances, but not to the small-scale fading parameters, we have not performed the SIC-ordering here and left it for future works. It has been shown in [5] that for an algorithm including N initial points, the exhaustive SIC ordering for a K users uplink-RSMA imposes a tolerable computational complexity of $\mathcal{O}(2^K + NK^3(2K!)/2^K)$.

$$\min_{\mathbf{X}} \left(\max_{1 \leq j \leq J} \{ \mathcal{F}_j \} \right), \quad (30)$$

$$\begin{aligned} \text{s.t. } C_1 : & \sum_{(k',n') \in \Phi_{m,k,n}} \log_2(p_{m,k',n'}) \leq \psi_k, \quad \forall k, n, & C_{2-1} : & \Gamma^{[t]}(D_{j,k,n}) \geq 1 + \theta_{j,k,n}, \quad \forall k, j, n, \\ C_{2-2} : & \theta_{j,k,n} \geq \frac{\text{PL}(d_{m,k,j})(2K_m-1)}{\sigma_e^2} \Theta^{[t]}(p_{m,k,n}, \varrho_{j,k,n}), \quad \forall k, j, n, \\ C_{2-3} : & \varrho_{j,k,n} \geq W_0 \left(\nu_{j,k,n}^{[t]} \left(1 - W_0 \left(\nu_{j,k,n}^{[t]} \right) \right) \right)^{-1} \left(\nu_{j,k,n} - \nu_{j,k,n}^{[t]} \right), \quad \forall k, j, n, \\ C_{2-4} : & \Psi^{[t]}(\nu_{j,k,n}, p_{m,k,n}^{2K_m}) \geq \frac{\sigma_e^2}{\text{PL}(d_{m,k,j})^{2K_m} (2K_m-1)} \vartheta_{j,k,n}, \quad \forall k, j, n, \\ C_{2-5} : & \log(\vartheta_{j,k,n}) \geq \frac{1}{(2K_m-1)} \left(\sum_{(k',n') \neq (k,n)} \Lambda^{[t]}(\zeta_{j,k',n'}) - \log(\epsilon_{\text{sop}}) \right), \quad \forall k, j, n, \\ C_3 : & r_{m,k,n}^* \geq D_{j,k,n}, \quad \forall k, n, & C_4 : & \sum_{n=1}^2 p_{m,k,n} \leq P_{m,k}, \quad \forall k. \end{aligned}$$

$$\begin{aligned} & \{p_{m,k,1}^*, D_{j,k,1}^*, p_{m,k,2}^*, D_{j,k,2}^*\} \text{ obtained from (30)} \\ & \quad \quad \quad \downarrow \uparrow \\ \text{update } r_{m,k,n}^{*[q+1]} &= \log_2 \left(1 + \frac{2A}{\sigma_m^2} W_0 \left(\left[\xi \epsilon_{\text{cop}}^{-1} \prod_{(k',n') \in \Phi_{m,k,n}} \left(2\lambda_{m,k',n'}^{*-1} \right) \right]^{\frac{1}{A}} \right) \right), \quad (31) \end{aligned}$$

and runs until $|r_{m,k,n}^{*[q+1]} - r_{m,k,n}^{*[q]}| \leq \epsilon$ is met or the maximum affordable number of iterations Q_{max} is reached. To find the ϵ -constraint solution $\{p_{m,k,1}^*, p_{m,k,2}^*, D_{j,k,n}^*\}$, the problem ((30)) is solved using the classic SPCA in another iterative process of the inner loop. In particular, the inner iterations are continued until the stopping criterion of $|\mathcal{F}_j^{[t+1]} - \mathcal{F}_j^{[t]}| \leq \delta_I^6$ is satisfied at the $(t+1)^{\text{st}}$ iteration or the maximum affordable number of iterations T_{max} is reached. The proposed two-tier scheme is presented in Algorithm I.

C. Complexity Analysis

In Algorithm 1, the major complexity lies in solving problem (30). According to Algorithm 1, a globally near-optimal solution of problem (30) is obtained via solving a series of convex problems with different initial points and decoding order strategies. Considering that the dimension of the variables in problem (30) is $\mathcal{L}_m = 5(1+J)K_m$, the

worst-case complexity order of solving the convex problem in Step 2 of inner-loop by using the standard interior point method is given by $\mathcal{O}\left(\left(\frac{\mathcal{L}_m-1}{2}\right)^3\right)$ [32, Pages 487, 569]. Since each cluster consists of K_m users and each user transmits a superposition of two messages (there are $2K_m$ messages for the m^{th} cluster), the decoding order set Π_m consists of $\frac{(2K_m)!}{2^{2K_m}}$ elements. Therefore, the total complexity of solving problem (30) at each iteration is given by $\mathcal{O}\left(\left(\frac{\mathcal{L}_m-1}{2}\right)^3 \frac{(2K_m)!}{2^{2K_m}}\right)$. In practice, we consider small K_m to reduce the SIC complexity, so that the computational complexity of Algorithm 1 remains practical. To deal with a large number of users, we can increase the number of clusters and the users can be classified into different clusters, each having a small number of users.

D. Convergence Analysis

In this section we establish a convergence analysis for the SPCA algorithm. Since the original problem (15) is non-convex, it is not possible to prove convergence to a global minimum but rather convergence to KKT points under some regularity

6

Note that $\mathcal{F}_j^{[t]}$ represents the value of \mathcal{F}_j at iteration t^{th} .

Algorithm 1 : Secure resource allocation proposed for the RSMA uplink

For $\Phi_m \in \Pi_m$ do:

 Call **Function Outer_Loop**

End.

Obtain the optimal solution $\left\{ p_{m,k,1}^*, D_{j,k,1}^*, p_{m,k,2}^*, D_{j,k,2}^* \right\}_{k=1}^{K_m}$, $\left\{ r_{m,k,1}^*, r_{m,k,2}^* \right\}_{k=1}^{K_m}$ and optimal decoding order $\Phi_m^* = \Phi_m$ with the highest OF.

Function Outer_Loop

Step 1: Initialize the maximum number of iterations Q_{max} , T_{max} and the maximum tolerance ϵ .

Step 2: Initialize $\left\{ r_{m,k,1}^{*[0]}, r_{m,k,2}^{*[0]} \right\}$ and the outer iteration index $q = 0$.

While $\left(\left| r_{m,k,n}^{*[q+1]} - r_{m,k,n}^{*[q]} \right| \geq \epsilon \text{ or } q \leq Q_{max} \right) \quad \forall k, n$, do:

 Step 3: Call the **Function Inner_Loop** with

$\left\{ r_{m,k,1}^{*[q]}, r_{m,k,2}^{*[q]} \right\}$ to obtain the ϵ -constraint solution $\left\{ p_{m,k,1}^*, D_{j,k,1}^*, p_{m,k,2}^*, D_{j,k,2}^* \right\}$.

 Step 4: Update $r_{m,k,n}^{*[q+1]}$ in (18).

 Step 5: **Goto** Step 3.

end while.

Step 6: Return the ϵ -constraint solution $\left\{ p_{m,k,1}^*, D_{j,k,1}^*, p_{m,k,2}^*, D_{j,k,2}^* \right\}$, $r_{m,k,1}^* = r_{m,k,1}^{*[q+1]}$ and $r_{m,k,2}^* = r_{m,k,2}^{*[q+1]}$.

Function Inner_Loop $\left(\left\{ r_{m,k,1}^{*[q+1]}, r_{m,k,2}^{*[q+1]} \right\} \right)$

Step 1: Initialize the inner iteration index $t = 0$, $\left\{ p_{m,k,1}^{[0]}, D_{j,k,1}^{[0]}, p_{m,k,2}^{[0]}, D_{j,k,2}^{[0]} \right\}$.

While $\left(\left| \mathcal{F}_j^{[t+1]} - \mathcal{F}_j^{[t]} \right| \geq \delta_I \text{ or } t \leq T_{max} \right)$ do:

 Step 2: Find the ϵ -constraint solution

$\left\{ p_{m,k,1}^{[t+1]}, D_{j,k,1}^{[t+1]}, p_{m,k,2}^{[t+1]}, D_{j,k,2}^{[t+1]} \right\}$ of the following problem

 for given $\left\{ p_{m,k,1}^{[t]}, D_{j,k,1}^{[t]}, p_{m,k,2}^{[t]}, D_{j,k,2}^{[t]} \right\}$, and $r_{m,k,n}^{*[m]}$

$\left\{ p_{m,k,1}^{[t+1]}, D_{j,k,1}^{[t+1]}, p_{m,k,2}^{[t+1]}, D_{j,k,2}^{[t+1]} \right\} = \text{Solving (30)}$,

 Step 3: Update $\mathcal{F}_j^{[t+1]}$.

 Step 4: **Goto** Step 2.

end while.

Step 5: Return $\left\{ p_{m,k,1}^*, D_{j,k,1}^*, p_{m,k,2}^*, D_{j,k,2}^* \right\} = \left\{ p_{m,k,1}^{[t+1]}, D_{j,k,1}^{[t+1]}, p_{m,k,2}^{[t+1]}, D_{j,k,2}^{[t+1]} \right\}$.

conditions. We use the following simple and technical lemmas will be used in the convergence proof. For simplicity we define $\Omega \triangleq$ feasible set of (15), $\Omega^{[t]} \triangleq$ feasible set of (30)⁷ for t^{th} iteration.

Lemma 1. Let $\mathcal{D} : \mathbb{R}^n \rightarrow \mathbb{R}$ be a strictly convex and differentiable function on a nonempty convex set $S \subseteq \mathbb{R}^n$. Then \mathcal{D} is strongly convex on the set S .

Proof: See [34]. ■

Lemma 2. Suppose $\{\mathbf{X}^{[t]}\}$ be the sequence generated by the SPCA method. Then for every $t \geq 0$: **i).** $\Omega^{[t]} \subseteq \Omega$, **ii).** $\mathbf{x}^{[t]} \in \Omega^{[t]} \cap \Omega^{[t+1]}$, **iii).** $\mathbf{X}^{[t]}$ is a feasible point of (15), **iv).** $\mathcal{F}_j^{[t+1]} \leq \mathcal{F}_j^{[t]}$.

Proof: See [34]. ■

Lemma 3. The sequence $\{\mathcal{F}_j^{[t]}\}$ converges.

Proof: See [34]. ■

Recall that a feasible solution \mathbf{X}^\otimes of a optimization problem is *regular* if the set of gradients of the active constraints at \mathbf{X}^\otimes is linearly independent [35]. If $\mathbf{X}^{[t]}$ converges to a regular point \mathbf{X}^\otimes , then \mathbf{X}^\otimes is a KKT point of problem (15). By Lemma2 it follows that the strictly convex objective function \mathcal{F}_j is also strongly convex on the convex feasible set $\Omega^{[t+1]}$. In particular, there exists $\vartheta > 0$ such that for all $k \geq 0$ we have:

$$\mathcal{F}_j^{[t]} - \mathcal{F}_j^{[t+1]} \geq \left(\mathbf{X}^{[t]} - \mathbf{X}^{[t+1]} \right)^T \nabla \mathcal{F}_j^{[t+1]} + \vartheta \left\| \mathbf{X}^{[t]} - \mathbf{X}^{[t+1]} \right\|^2, \quad (32)$$

In this paper, we consider the standard form of generic optimization problem as follow [36]:

$$\begin{aligned} & \min f(\mathbf{x}) \\ & \text{s.t. } c_j(\mathbf{x}) \leq 0, \quad \forall j = 1, 2, \dots, m \\ & \quad \mathbf{x} \in \mathbb{R}^n \end{aligned}$$

where $f(\mathbf{x})$ and $c_j(\mathbf{x})$, $\forall j = 1, \dots, m$ are all continuously differentiable objective and constraint functions over \mathbb{R}^n , respectively. Also, we assume that the function $f(\mathbf{x})$ and the last $m - p$ constraint functions $c_{p+1}(\mathbf{x}), \dots, c_m(\mathbf{x})$ ($p \leq m$) are convex over \mathbb{R}^n . Therefore, the “non-convex part” of the problem is due to the nonconvexity of the first p constraint functions $c_1(\mathbf{x}), \dots, c_p(\mathbf{x})$. The case $p = m$ corresponds to the case when all the constraints are non-convex. In addition, suppose that for every $j = 1, \dots, p$, $c_j(\mathbf{x})$ has a continuous convex upper estimate function $C_j : \mathbb{R}^n \times \mathbb{Y} \rightarrow \mathbb{R}$, specifically, assume that there exists a set $\mathbb{Y} \subseteq \mathbb{R}^r$ (r is a positive integer), such that $c_j(\mathbf{x}) \leq C_j(\mathbf{x}, \boldsymbol{\rho})$, $\forall \mathbf{x} \in \mathbb{R}^n$, $\forall \boldsymbol{\rho} \in \mathbb{Y}$, where for a fixed $\boldsymbol{\rho}$ the function $C_j(\cdot, \boldsymbol{\rho})$ is convex and continuously differentiable. The basic idea of SPCA is that at each iteration i , we replace each non-convex functions $c_j(\mathbf{x})$, $\forall j = 1, \dots, p$ by the upper convex approximation function $C_j(\mathbf{x}, \boldsymbol{\rho})$ for some appropriately chosen parameter vector $\boldsymbol{\rho}$. Thus, at step i ($i \geq 1$) we need to solve the following equivalent convex problem:

$$\begin{aligned} & \min f(\mathbf{x}) \\ & \text{s.t. } C_j(\mathbf{x}, \boldsymbol{\rho}) \leq 0, \quad \forall j = 1, 2, \dots, p \\ & \quad c_i(\mathbf{x}) \leq 0, \quad \forall j = p + 1, p + 2, \dots, m \\ & \quad \mathbf{x} \in \mathbb{R}^n \end{aligned}$$

since $\mathbf{X}^{[t]}$ is a feasible point of (30) (by Lemma 3), and $\mathbf{X}^{[t+1]}$ is its optimum, then from the optimality conditions for $(t+1)^{th}$ iteration of (30) (see [36, proposition 2.1.2]), we obtain $(\mathbf{X}^{[t]} - \mathbf{X}^{[t+1]})^\top \nabla \mathcal{F}_j^{[t+1]} \geq 0$, which combined with (32) yields:

$$\mathcal{F}_j^{[t]} - \mathcal{F}_j^{[t+1]} \geq \vartheta \|\mathbf{X}^{[t]} - \mathbf{X}^{[t+1]}\|^2 \quad (33)$$

By Lemma 3, the sequence $\{\mathcal{F}_j^{[t]}\}$ converges and thus the inequality (33) implies that $\|\mathbf{X}^{[t]} - \mathbf{X}^{[t+1]}\| \rightarrow 0$. Let be $\mathbf{X}^\diamond \triangleq (\mathbf{x}^\diamond, \{p_{m,k,1}^\diamond, D_{j,k,1}^\diamond, p_{m,k,2}^\diamond, D_{j,k,2}^\diamond\}_{k=1}^{K_M})$ an accumulation point of the sequence $\{\mathbf{X}^{[t]}\}$, we will show that \mathbf{X}^\diamond is a KKT point. Since \mathbf{X}^\diamond is an accumulation point of $\{\mathbf{X}^{[t]}\}$, there exists a subsequence $\{\mathbf{X}^{[t_n]}\}$ such that $\mathbf{X}^{[t_n]} \rightarrow \mathbf{X}^\diamond$ when the iteration number $n \rightarrow \infty$. Regarding the limit point \mathbf{X}^\diamond , we can make the following statement.

Corollary 4. *The accumulation point \mathbf{X}^\diamond of the sequence $\{\mathbf{X}^{[t]}\}$ generated by the proposed SPCA method is a KKT point of the (30).*

Proof: We know from [35] that there exist Lagrangian multipliers λ_i^* together with the accumulation point \mathbf{X}^\diamond that satisfy the following KKT's necessary and sufficient condition for optimality of convex problem [35, Sec 5.5], at (34) $\{\gamma_i\}_{i=1}^8$ denote the lagrangian multipliers of problem (30). If we choose $\gamma_i = \lambda_i$ for $i = 1, \dots, 8$ we conclude that the point \mathbf{X}^\diamond also satisfy so, we proved that if the sequence $\{\mathbf{X}^{[t]}\}$ generated by the SPCA method converges to a regular point \mathbf{X}^\diamond , then \mathbf{X}^\diamond is a KKT point of the SPCA problem (30). It has already been shown that the point \mathbf{X}^\diamond is a KKT point (stationary point) of the SPCA problem (30). This stationary point cannot be saddle point, since the objective function \mathcal{F}_j is strictly convex function and twice-continuously differentiable in the variable \mathbf{X} . By a simple contradiction method, we can also show that the point \mathbf{X} cannot be a local maximum [35]. ■

V. SIMULATION RESULTS

In this section, we evaluate the secure transmission performance of the proposed algorithm through simulations. Each point in the figures is obtained by averaging over 150 simulation trials. Unless otherwise specified, the simulation setup

is as follows throughout this section. In the scenario investigated a UAV hovers above the users to provide communication services. Explicitly, the UAV has a coverage radius of $R_{UAV} = 800$ m and altitude of $H_i = 140$ m. The path-loss model in the UAV network includes both LoS and non-LoS links associated with the path-loss exponents of $\mathcal{L}_{m,k} = 2$ and $\mathcal{N}_{m,k} = 3.5$, respectively. There are $M = 3$ clusters, 100 users associated with $P_{i,k} = \frac{P}{\sum_{m=1}^M K_m}$, where P is the total power budget, and $J = 3$ *Eves* randomly distributed in the whole system between 1 m and 800 m. Once the large-scale fading parameters are generated, they are assumed to be known and fixed throughout the simulations. The small-scale fading vectors of all users and *Eves* are independently generated according to $\mathcal{CN}(0, \mathbf{I}_{N_t})$. The noise power at each user and eavesdropper is set to $\sigma_m^2 = \sigma_e^2 = 0$ dB. Moreover, we set $T_{max} = Q_{max} = 20$, $N_t = 5$, $\epsilon_{cop} = \epsilon_{sop} = 0.1$, and the maximum threshold value used for the termination of Algorithm 1 is set to $\delta_I = 10^{-2}$. The maximum tolerance of $\epsilon = 10^{-3}$ is assumed for the termination criterion used in Algorithm 1.

Firstly, in Fig. 4 we demonstrate the convergence of Algorithm 1 is solving (18) and (19) for different values of P . The convergence of the inner loop of Algorithm 1 in terms of updating $\mathcal{F}_j^{[t]}$ is shown by black-lines. It is observed that the inner loop converges within 6 iterations for different values of P , which corroborates the convergence of (30). When fixing the number of users, the power $P_{i,k}$ allocated to each user increases upon increasing P . As a result, the OF value of $\mathcal{F}_j^{[t]}$ in (30) increases as P increases. On the other hand, the convergence of the outer loop of Algorithm 1 is characterized by the red-lines. Observe that the algorithm used for solving (18) converges after a maximum of 10 iterations under different values of P . Fig. 5 shows the ENST of the proposed scheme versus J for different values of ϵ_{cop} . Naturally, upon increasing J , the performance degrades due to having more *Eves* in the system, but using a higher ϵ_{cop} would increase ENST and compensate for the performance loss. Additionally, as another important observation, without performing SIC at *Eve* (ESIC), the *Eve*'s rate is increased, resulting in ENST enhancement.

To show the performance advantages of the proposed scheme by employing the RSMA scheme, we compare it to both power-domain (PD) NOMA

$$\begin{aligned}
& \nabla \mathcal{F}_j + \gamma_1 \nabla \left(\sum_{(k',n') \in \Phi_{m,k,n}} \log_2(p_{m,k',n'}) - \psi_k \right) + \gamma_2 \nabla \left(1 + \theta_{j,k,n} - \Gamma^{[t]}(D_{j,k,n}) \right) + \gamma_3 \nabla \left(\frac{\text{PL}(d_{m,k,j})(2K_m - 1)}{\sigma_e^2} \right) \\
& + \Theta^{[t]}(p_{m,k,n}, \varrho_{j,k,n}) - \theta_{j,k,n} \Big) + \gamma_4 \nabla \left(W_0 \left(\nu_{j,k,n}^{[t]} \right) \left(\nu_{j,k,n}^{[t]} \left(1 - W_0 \left(\nu_{j,k,n}^{[t]} \right) \right) \right)^{-1} \left(\nu_{j,k,n} - \nu_{j,k,n}^{[t]} \right) - \varrho_{j,k,n} \right) + \\
& \gamma_5 \nabla \left(\frac{\sigma_e^2}{\text{PL}(d_{m,k,j})^{2K_m} (2K_m - 1)} \vartheta_{j,k,n} - \Psi^{[t]} \left(\nu_{j,k,n}, p_{m,k,n}^{2K_m} \right) \right) + \gamma_6 \nabla \left(D_{j,k,n} - r_{m,k,n}^* \right) + \\
& \gamma_7 \nabla \left(\frac{1}{(2K_m - 1)} \left(\sum_{(k',n') \neq (k,n)} \Lambda^{[t]}(\zeta_{j,k',n'}) - \log(\epsilon_{\text{SOP}}) \right) - \log(\vartheta_{j,k,n}) \right) + \gamma_8 \nabla \left(\sum_{n=1}^2 p_{m,k,n} - P_{m,k} \right) = 0. \quad (34)
\end{aligned}$$

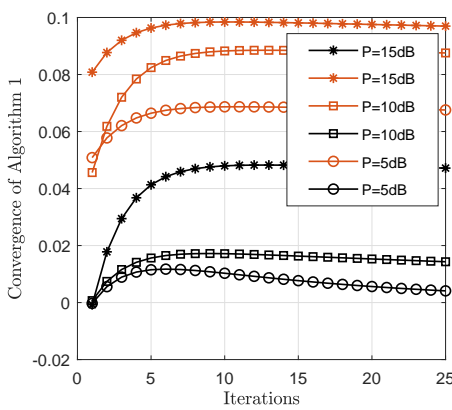


Fig. 4. The Convergence of Algorithm 1, black-line refer to $\mathcal{F}_j^{[t]}$ and red-line refer to $r_{m,k,n}^{*[q]}$ for different values of P .

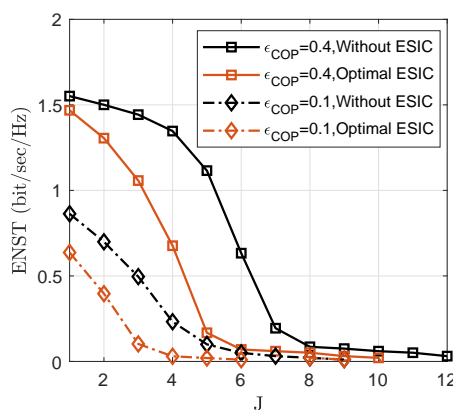


Fig. 5. ENST versus J for different values of ϵ_{COP} and with/without optimal Eve SIC ordering.

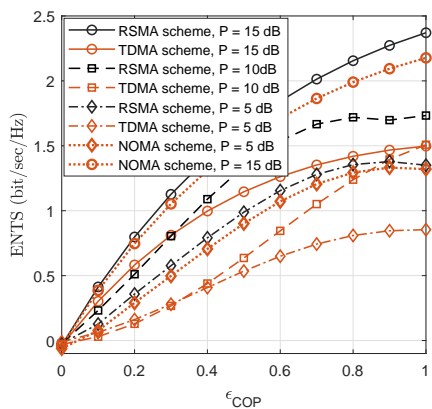


Fig. 6. ENST versus ϵ_{COP} for different values of P .

and TDMA. In PD-NOMA, the UAV first decodes the messages of users having high channel gains and then decodes the messages of users with low channel gains by subtracting the interference imposed by the previously decoded high-gain user. In TDMA, each user will be assigned a fraction of time to use the whole bandwidth. Let $\alpha_{m,k} = \frac{1}{K_m}$ be the fraction of time allocated to $U_{m,k}$. Then the data rate of $U_{m,k}$ becomes $C_{m,k}^{\text{TDMA}} = \alpha_{m,k} \log_2 \left(1 + \frac{p_{m,k,n} |w_m^H \mathbf{h}_{m,k}|^2}{\sigma_m^2} \right)$. Observe from Fig. 6 that RSMA always achieves a better performance than PD-NOMA and TDMA. Moreover, the ENST gain of the proposed scheme over TDMA becomes more prominent as P and ϵ_{COP} increases.

The corresponding ENST versus ϵ plot is provided in Fig. 7, where the proposed scheme achieves a significantly higher ENST upon increasing P , ϵ_{SOP} and ϵ_{COP} . A heuristic explanation of this phe-

nomenon is that increasing both the connection and secrecy outage threshold tends to relax the constraints of (30), and decrease the lower bound of (19)- C_2 , which in turn increases the ENST.

Finally, to show the importance of considering SIC ordering as well as imperfect CSIT, we compare the proposed scheme for both optimal SIC (OSIC) and Sub-optimal SIC (SSIC) ordering. Additionally, we also consider RSMA with perfect CSIT. To make a fair comparison, we simulate all schemes under the same security requirement. The ENST versus P trends recorded for different values of ϵ_{COP} are provided in Fig. 8, where the proposed scheme always achieves significantly higher ENST than RSMA ignoring CSIT uncertainty. Fig. 8 suggests that using bigger ϵ_{COP} would increase the ENST and mitigate the performance loss of SSIC.

Finally, Fig. 9 illustrates the ENST versus N_e . This figure indicates that increasing the number of

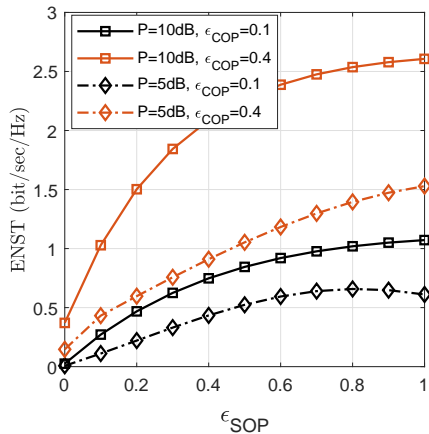


Fig. 7. ENST versus ϵ_{sop} for different values of P and ϵ_{cop} .

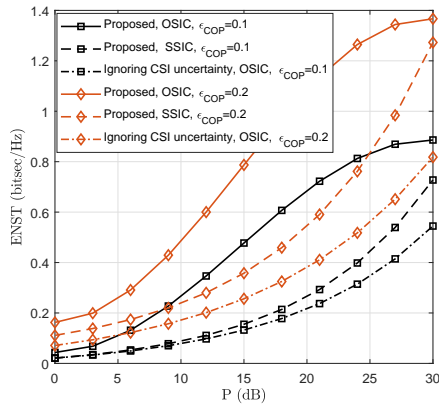


Fig. 8. ENST versus P for different values of ϵ_{cop} and SIC method.

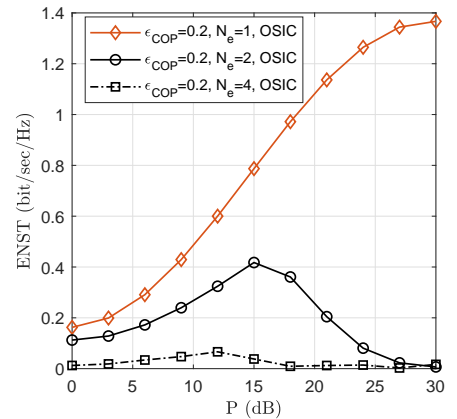


Fig. 9. ENST versus ϵ_{cop} for different values of N_e .

the receive antennas at *Eve*, the system's secrecy performance is degraded due to *Eve*'s improved ability to eavesdrop and infer from common message. Interestingly, our proposed scheme still shows considerable robustness against a multiple antenna-aided *Eve*, hence we can achieve non-zero ENST.

VI. CONCLUSIONS

In this article, we proposed secure RSMA uplink transmission under imperfect CSIT for a UAV-BS network, in which RSMA is employed by each legitimate users for secure transmission under large-scale uplink access. To characterize the performance of this system, an efficient block coordinate decent algorithm was proposed for maximizing the effective network secrecy throughput under the constraints of secrecy and the reliability outage probabilities and transmit power budget constraints. To solve this problem, we derived the closed-form optimal RS rate expression of each user. Then, the ϵ -constraint transmit power of each user was calculated by the classic SPCA technique under a given decoding order and then the optimal decoding order was found by an exhaustive search method. Numerical results demonstrated that the proposed algorithm significantly improves the effective network secrecy throughput compared to the PD-NOMA and TDMA benchmarks, as well as to the RSMA transmission ignoring CSIT uncertainty.

APPENDIX A DERIVATION OF (12)

Based on (9), $P_{m,k,n}^{CO}$ can be expressed as A1, where we have $\mathcal{X}_k \triangleq |\mathbf{w}_m^H \mathbf{f}_{m,k}|^2 \geq 0$, $\mathcal{Y}_{i,k''} \triangleq \|\mathbf{f}_{i,k''}\|^2 \sin^2(\phi_{i,k''}) |\mathbf{w}_m^H \mathbf{e}_{i,k''}|^2 \geq 0$. Otherwise, $P_{m,k}^{CO}$ is always one. Furthermore, based on the independence of the interference terms [7, eq 24], the variables $\{\mathcal{X}_k\}$ and $\{\mathcal{Y}_{i,k''}\} \forall i, k, k''$ are indeed independent.

To obtain a closed-form expression of $P_{m,k}^{CO}$, we first provide the probability density function (pdf) of \mathcal{X}_k . Recall that $\mathbf{n}_{m,k} \sim \mathcal{CN}(0, \mathbf{I}_{N_t})$ and $\tilde{\mathbf{f}}_{m,k} \triangleq \frac{\mathbf{f}_{m,k}}{\|\mathbf{f}_{m,k}\|}$, \mathcal{X}_k can be rewritten as $\mathcal{X}_k = \|\mathbf{f}_{m,k}\|^2 |\mathbf{w}_m^H \tilde{\mathbf{f}}_{m,k}|^2$. Since the normalized beamformer weights \mathbf{w}_m are determined by $\{\mathbf{v}_i\}_{i=1, i \neq m}^M$ according to $\mathbf{w}_m^H \mathbf{v}_l = 0, \forall l \neq m$, and $\{\mathbf{v}_i\}_{i=1, i \neq m}^M$ are independent of $\mathbf{f}_{m,k}$, the vectors $\mathbf{f}_{m,k}$ and \mathbf{w}_m are also independent. As a result, $\mathbf{f}_{m,k}$ and \mathbf{w}_m are independent unit-norm vectors in the N_t -dimensional space. Based on [27, Lemma 1], the square inner product between two independent unit-norm random vectors is Beta distributed with shape parameters of $(1, N_t - 1)$, i.e., we have $X_1 \triangleq |\mathbf{w}_m^H \tilde{\mathbf{f}}_{m,k}|^2 \sim \text{Beta}(1, N_t - 1)$ and its pdf is $f_{X_1}(x_1) = \frac{(1-x_1)^{N_t-2}}{\text{Be}(1, N_t-1)}$, $x_1 \in [0, 1]$ [29, eq 8.380]. On the other hand, since we have $\mathbf{f}_{m,k} \sim \mathcal{CN}(0, \mathbf{I}_{N_t})$, $X_2 \triangleq \|\mathbf{f}_{m,k}\|^2$ is distributed as a chi-squared r.v. with $2N_t$ degrees of freedom as $\chi_{2N_t}^2$, and its pdf is $f_{X_2}(x_2) = \frac{x_2^{N_t-1} e^{-\frac{x_2}{2}}}{2^{N_t} \Gamma(N_t)}$, $x_2 \geq 0$, where $\Gamma(x)$ is the Gamma

$$\mathbb{P} \left\{ 2^{r_{m,k,n}} - 1 > \frac{p_{m,k,n} \text{PL}(d_{m,k}) |\mathbf{w}_m^H \mathbf{f}_{m,k}|^2}{\sum_{(k',n') \in \Phi_{m,k,n}} p_{m,k',n'} \text{PL}(d_{m,k'}) |\mathbf{w}_m^H \mathbf{f}_{m,k'}|^2 + \sum_{i=1, i \neq m}^M \sum_{k''=1}^{K_i} P_{i,k''} \text{PL}(d_{i,k''}) \|\sin(\phi_{i,k''}) \mathbf{f}_{i,k''}\|^2 |\mathbf{w}_m^H \mathbf{e}_{i,k''}|^2 + \sigma_m^2} \right\}$$

$$= \mathbb{P} \left\{ 2^{r_{m,k,n}} - 1 > \frac{p_{m,k,n} \text{PL}(d_{m,k}) \mathcal{X}_k}{\sum_{(k',n') \in \Phi_{m,k,n}} p_{m,k',n'} \text{PL}(d_{m,k'}) \mathcal{X}_{k'} + \sum_{i=1, i \neq m}^M \sum_{k''=1}^{K_i} P_{i,k''} \text{PL}(d_{i,k''}) \mathcal{Y}_{i,k''} + \sigma_m^2} \right\}, \quad (\text{A1})$$

function [50, eq. 8.310]. Since $\mathcal{X}_k = X_1 X_2$, and X_1 and X_2 are independent, the pdf of \mathcal{X}_k is given by:

$$f_{\mathcal{X}_k}(x) = \int_x \frac{1}{|x_2|} f_{X_2}(x_2) f_{X_1}\left(\frac{x}{x_2}\right) dx_2$$

$$= \frac{\int_x^{+\infty} (x_2 - x)^{N_t - 2} e^{-\frac{x_2}{2}} dx_2}{\text{Be}(1, N_t - 1) 2^{N_t} \Gamma(N_t)}$$

$$= \frac{1}{2} e^{-\frac{x}{2}}, x \geq 0 = \text{Exp}\left(\frac{1}{2}\right). \quad (\text{A2})$$

Thus, $\mathcal{X}_k \sim \text{Exp}(\frac{1}{2})$ is exponentially distributed with rate $\lambda_k = \frac{1}{2}$. Now, we derive the pdf of $\mathcal{Y}_{i,k''}$. The cumulative distribution function of $\Omega_{i,k''} \triangleq \sin^2(\phi_{i,k''})$ is given by [30]:

$$F_{\Omega_{i,k''}}(\varpi) = \begin{cases} 1, & \text{if } 0 \leq \varpi \leq 2^{-\frac{B}{N_t-1}}, \\ 2^B (\varpi)^{N_t-1}, & \text{if } \varpi \geq 2^{-\frac{B}{N_t-1}}. \end{cases} \quad (\text{A3})$$

Hence, we have $\|\mathbf{f}_{i,k''}\|^2 \sin^2(\phi_{i,k''}) \sim \text{Gamma}(N_t - 1, 2^{-\frac{B}{N_t-1}})$, which is gamma distributed with a shape parameter of $N_t - 1$ and scale parameter of $2^{-\frac{B}{N_t-1}}$ [30, Lemma 1]. On the other hand, $\mathbf{e}_{i,k''}$ is a unit vector that has the same distribution as $\mathbf{f}_{i,k''}$. Moreover, the unit vector \mathbf{w}_m is isotropic within the $(N_t - 1)$ -dimensional hyperplane and independent of $\mathbf{e}_{i,k''}$. Based on [25, Lemma 2], we have $|\mathbf{w}_m^H \mathbf{e}_{i,k''}|^2 \sim \text{Beta}(1, N_t - 2)$. Therefore the product $\mathcal{Y}_{i,k''} = \text{Beta}(1, N_t - 2) \times \text{Gamma}(N_t - 1, 2^{-\frac{B}{N_t-1}})$ is exponentially distributed as [31, Lemma 1], $\mathcal{Y}_{i,k''} = \|\mathbf{f}_{i,k''}\|^2 \sin^2(\phi_{i,k''}) |\mathbf{w}_m^H \mathbf{e}_{i,k''}|^2 \sim \text{Exp}(2^{\frac{B}{N_t-1}})$. If we define the new variables

$$\bar{\mathcal{X}}_{m,k',n'} \sim \text{Exp}\left(\lambda_{m,k',n'} = \frac{1}{2p_{m,k',n'} \text{PL}(d_{m,k'})}\right),$$

$$\bar{\mathcal{Y}}_{i,k''} \sim \text{Exp}\left(\lambda_{i,k''} = \frac{2^{\frac{B}{N_t-1}}}{P_{i,k''} \text{PL}(d_{i,k''})}\right),$$

then the $PCO_{m,k,n}$ can be expressed as (A4), where $\mathcal{L}_X(s) \triangleq \mathbb{E}\{e^{-sx}\}$ is the Laplace transform. Step (a) is reached by conditioning on the aggregate interference $\sum_{(k',n') \in \Phi_{m,k,n}} \bar{\mathcal{X}}_{m,k',n'} + \sum_{i=1, i \neq m}^M \sum_{k''=1}^{K_i} \bar{\mathcal{Y}}_{i,k''}$ and (b) by

the independence of the interference terms.

APPENDIX B DERIVATION OF (13)

Based on (10), $P_{j,k,n}^{SO}$ can be expressed as (B1), where $\mathcal{W}_{j,k,n} \triangleq p_{m,k,n} \text{PL}(d_{m,k,j}) \lambda_j^{max} \{\tilde{\mathcal{Q}}_{m,j}\} |g_{m,k,j}|^2$ and $\mathcal{U}_{j,k',n'} \triangleq p_{m,k',n'} \text{PL}(d_{m,k',j}) \lambda_j^{max} \{\tilde{\mathcal{Q}}_{m,j}\} |g_{m,k',j}|^2$ are independent exponential r.v obeying the distribution of $\mathcal{W}_{j,k,n} \sim \text{Exp}\left(\eta_{j,k,n} = \frac{1}{p_{m,k,n} \text{PL}(d_{m,k,j}) \lambda_j^{max} \{\tilde{\mathcal{Q}}_{m,j}\}}\right)$ and $\mathcal{U}_{k',n'} \sim \text{Exp}\left(\zeta_{j,k',n'} = \frac{1}{p_{m,k',n'} \text{PL}(d_{m,k',j}) \lambda_j^{max} \{\tilde{\mathcal{Q}}_{m,j}\}}\right)$.

Then the $P_{j,k,n}^{SO}$ can be expressed as (B2), where $\kappa_{j,k,n} \triangleq 2^{D_{j,k,n}} - 1$.

APPENDIX C DERIVATION OF (14)

Upon using the inequality of $\frac{1}{1+x} \leq \frac{1}{x}$ we have (C1) and (C2).

The first-order derivative of $\Psi(\kappa_{j,k,n})$ is given by (C3), which is negative. By exploiting the decreasing nature of $\Psi(\kappa_{j,k,n})$ and its lower-bounded nature in (C2), the minimum value of $D_{j,k,n}$ is obtained by solving the (C4). By straightforward algebra, (C4) can be further reformulated as (C5). Finally, with the help of the principal branch of the Lambert W -function [19], (C5) is rewritten as (C6). Re-arranging the terms in (C6) leads to (14).

REFERENCES

- [1] M. Alzenad, A. El-Keyi, and H. Yanikomeroglu, "3-D placement of an unmanned aerial vehicle base station for maximum coverage of users with different QoS requirements," *IEEE Wireless Communications Letters*, vol. 7, no. 1, pp. 38–41, 2017.
- [2] Y. Sun, D. Xu, D. W. K. Ng, L. Dai and R. Schober, "Optimal 3D-Trajectory Design and Resource Allocation for Solar-Powered UAV Communication Systems," *in IEEE Transactions on Communications*, vol. 67, no. 6, pp. 4281–4298, June 2019, doi: 10.1109/TCOMM.2019.2900630.

$$\begin{aligned}
P_{m,k,n}^{CO} &= 1 - \mathbb{P} \left\{ \beta_{m,n,k} \leq \frac{\bar{\mathcal{X}}_{m,k,n}}{\sum_{(k',n') \in \Phi_{m,k,n}} \bar{\mathcal{X}}_{m,k',n'} + \sum_{i=1, i \neq m}^M \sum_{k''=1}^{K_i} \bar{\mathcal{Y}}_{i,k''} + \sigma_m^2} \right\} \\
&= 1 - \mathbb{P} \left\{ \bar{\mathcal{X}}_{m,k,n} \geq \beta_{m,n,k} \left(\sum_{(k',n') \in \Phi_{m,k,n}} \bar{\mathcal{X}}_{m,k',n'} + \sum_{i=1, i \neq m}^M \sum_{k''=1}^{K_i} \bar{\mathcal{Y}}_{i,k''} + \sigma_m^2 \right) \right\} \\
&\stackrel{(a)}{=} 1 - \mathbb{E} \left\{ \exp \left(- \frac{\beta_{m,n,k} \left(\sum_{(k',n') \in \Phi_{m,k,n}} \bar{\mathcal{X}}_{m,k',n'} + \sum_{i=1, i \neq m}^M \sum_{k''=1}^{K_i} \bar{\mathcal{Y}}_{i,k''} + \sigma_m^2 \right)}{2} \right) \right\} \\
&\stackrel{(b)}{=} 1 - \mathbb{E} \left\{ \exp \left(- \frac{\beta_{m,n,k} \sigma_m^2}{2} \right) \prod_{(k',n') \in \Phi_{m,k,n}} \mathcal{L}_{\bar{\mathcal{X}}_{m,k',n'}} \left(\frac{\beta_{m,n,k}}{2} \right) \prod_{i=1, i \neq m}^M \prod_{k''=1}^{K_i} \mathcal{L}_{\bar{\mathcal{Y}}_{i,k''}} \left(\frac{\beta_{m,n,k}}{2} \right) \right\} \\
&= 1 - \exp \left(- \frac{\beta_{m,n,k} \sigma_m^2}{2} \right) \prod_{(k',n') \in \Phi_{m,k,n}} \prod_{i=1, i \neq m}^M \prod_{k''=1}^{K_i} \left(\frac{\lambda_{m,k',n'}}{\lambda_{m,k',n'} + \frac{\beta_{m,n,k}}{2}} \right) \left(\frac{\lambda_{i,k''}}{\lambda_{i,k''} + \frac{\beta_{m,n,k}}{2}} \right), \quad (A4)
\end{aligned}$$

$$\begin{aligned}
P_{j,k,n}^{SO} &= \mathbb{P} \left\{ 2^{D_{j,k,n}} - 1 < \frac{p_{m,k,n} \text{PL}(d_{m,k,j}) |g_{m,k,j}|^2}{\sum_{(k',n') \neq (k,n)} p_{m,k',n'} \text{PL}(d_{m,k',j}) |g_{m,k',j}|^2 + \sigma_e^2} \right\} \quad (B1) \\
&= \mathbb{P} \left\{ 2^{D_{j,k,n}} - 1 < \frac{\mathcal{W}_{j,k,n}}{\sum_{(k',n') \neq (k,n)} \mathcal{U}_{j,k',n'} + \sigma_e^2} \right\},
\end{aligned}$$

$$\begin{aligned}
P_{j,k,n}^{SO} &= \mathbb{P} \left\{ \mathcal{W}_{j,k,n} > \kappa_{j,k,n} \left(\sum_{(k',n') \neq (k,n)} \mathcal{U}_{j,k',n'} + \sigma_e^2 \right) \right\} \stackrel{(a)}{=} \mathbb{P} \left\{ \exp \left(-\eta_{j,k,n} \kappa_{j,k,n} \left(\sum_{(k',n') \neq (k,n)} \mathcal{U}_{j,k',n'} + \sigma_e^2 \right) \right) \right\}, \quad (B2) \\
&\stackrel{(b)}{=} \mathbb{E} \left\{ \exp \left(-\eta_{j,k,n} \kappa_{j,k,n} \sigma_e^2 \right) \prod_{(k',n') \neq (k,n)} \mathcal{L}_{\mathcal{U}_{k',n'}} \left(\eta_{j,k,n} \kappa_{j,k,n} \right) \right\} = \exp \left(-\eta_{j,k,n} \kappa_{j,k,n} \sigma_e^2 \right) \prod_{(k',n') \neq (k,n)} \left(1 + \eta_{j,k,n} \kappa_{j,k,n} \zeta_{j,k',n'}^{-1} \right)^{-1},
\end{aligned}$$

- [3] W. Jaafar, N. Shima, M. Sami, C.S Paschalis, and H. Yanikomeroglu. "On the downlink performance of RSMA-based UAV communications." *IEEE Transactions on Vehicular Technology* 69, no. 12 (2020): 16258-16263.
- [4] H. Zhang, J. Zhang and K. Long, "Energy Efficiency Optimization for NOMA UAV Network with Imperfect CSI," in *IEEE Journal on Selected Areas in Communications*, vol. 38, no. 12, pp. 2798-2809, Dec. 2020, doi: 10.1109/JSAC.2020.3005489.
- [5] H. Bastami, M. Letafati, M. Moradikia, A. Abdelhadi, H. Behroozi and L. Hanzo, "On the Physical Layer Security of the Cooperative Rate-Splitting Aided Downlink in UAV Networks," in *IEEE Transactions on Information Forensics and Security*, doi: 10.1109/TIFS.2021.312298
- [6] H. Bastami, M. Moradikia, M. Letafati, A. Abdelhadi, and H. Behroozi. "Outage-Constrained Robust and Secure Design for Downlink Rate-Splitting UAV Networks." In *2021 IEEE International Conference on Communications Workshops (ICC Workshops)*, pp. 1-7. IEEE, 2021.
- [7] M. Kountouris, and J. G. Andrews. "Downlink SDMA with limited feedback in interference-limited wireless networks." *IEEE Transactions on Wireless Communications* 11, no. 8 (2012): 2730-2741.
- [8] Z. Li, M. Xia, M. Wen, and Y. Wu. "Massive access in secure NOMA under imperfect CSI: security guaranteed sum-rate maximization with first-order algorithm." *IEEE Journal on Selected Areas in Communications* 39, no. 4 (2020): 998-1014.
- [9] Y. Mao, B. Clerckx, and V. O. Li, "Rate-splitting multiple access for downlink communication systems: bridging, generalizing, and outperforming SDMA and NOMA," *EURASIP journal on wireless communications and networking*, vol. 2018, no. 1, p. 133, 2018.
- [10] H. Fu, S. Feng, W. Tang and D. W. K. Ng, "Robust Secure Beamforming Design for Two-User Downlink MISO Rate-Splitting Systems," in *IEEE Transactions on Wireless Communications*, vol. 19, no. 12, pp. 8351- 8365, Dec. 2020.
- [11] J. Zeng, T. Lv, W. Ni, R. P. Liu, N. C. Beaulieu and Y. J. Guo, "Ensuring Max-Min Fairness of UL SIMO-NOMA: A Rate Splitting Approach," in *IEEE Transactions on Vehicular Technology*, vol. 68, no. 11, pp. 11080-11093, Nov. 2019, doi: 10.1109/TVT.2019.2943511.

$$\exp\left(-\eta_{j,k,n}\kappa_{j,k,n}\sigma_e^2\right) \prod_{(k',n') \neq (k,n)} \left(1 + \eta_{j,k,n}\kappa_{j,k,n}\zeta_{j,k',n'}^{-1}\right)^{-1} \leq \Psi(\kappa_{j,k,n}) \leq \epsilon_{sop}, \quad (C1)$$

$$\Psi(\kappa_{j,k,n}) \triangleq \exp\left(-\eta_{j,k,n}\kappa_{j,k,n}\sigma_e^2\right) \kappa_{j,k,n}^{-(2K_m-1)} \frac{\prod_{(k',n') \neq (k,n)} \zeta_{j,k',n'}}{\eta_{j,k,n}}. \quad (C2)$$

$$\Psi'(\kappa_{j,k,n}) = -\kappa_{j,k,n}^{-(2K_m-1)} \left(\eta_{j,k,n}\sigma_e^2 + \frac{(2K_m-1)}{\kappa_{j,k,n}}\right) < 0, \quad \kappa_{j,k,n} > 0, \quad (C3)$$

$$\exp\left(-\eta_{j,k,n}\kappa_{j,k,n}\sigma_e^2\right) \kappa_{j,k,n}^{-(2K_m-1)} \frac{\prod_{(k',n') \neq (k,n)} \zeta_{j,k',n'}}{\eta_{j,k,n}} = \epsilon_{sop}. \quad (C4)$$

$$\frac{\eta_{j,k,n}\sigma_e^2}{(2K_m-1)} \kappa_{j,k,n} \exp\left(-\frac{\eta_{j,k,n}\sigma_e^2}{(2K_m-1)} \kappa_{j,k,n}\right) = \frac{\eta_{j,k,n}\sigma_e^2}{(2K_m-1)} \left(\frac{\prod_{(k',n') \neq (k,n)} \zeta_{j,k',n'}}{\eta_{j,k,n}} \epsilon_{sop}^{-1}\right)^{\frac{1}{(2K_m-1)}}. \quad (C5)$$

$$W_0 \left(\frac{\eta_{j,k,n}\sigma_e^2}{(2K_m-1)} \left(\frac{\prod_{(k',n') \neq (k,n)} \zeta_{j,k',n'}}{\eta_{j,k,n}} \epsilon_{sop}^{-1}\right)^{\frac{1}{(2K_m-1)}}\right) = \frac{\eta_{j,k,n}\sigma_e^2}{(2K_m-1)} \kappa_{j,k,n}. \quad (C6)$$

- [12] O. Abbasi, and H. Yanikomeroglu, "Rate-Splitting and NOMA-Enabled Uplink User Cooperation." *In 2021 IEEE Wireless Communications and Networking Conference Workshops (WCNCW)* (pp. 1-6). IEEE, 2021.
- [13] Z. Yang, M. Chen, W. Saad, W. Xu, and M. Shikh-Bahaei. "Sum-rate maximization of uplink rate splitting multiple access (RSMA) communication." *IEEE Transactions on Mobile Computing (2020)*.
- [14] S. -. Lin, T. -. Chang, Y. -. Hong and C. -. Chi, "On the Impact of Quantized Channel Direction Feedback in Multiple-Antenna Wiretap Channels," *2010 IEEE International Conference on Communications*, 2010, pp. 1-5, doi: 10.1109/ICC.2010.5502608.
- [15] M. Moradikia, H. Bastami, A. Kuhestani, H. Behroozi, and L. Hanzo, "Cooperative secure transmission relying on optimal power allocation in the presence of untrusted relays, a passive eavesdropper and hardware impairments," *IEEE Access*, vol. 7, pp. 116 942–116 964, 2019.
- [16] M. Moradikia, S. Mashdour, and A. Jamshidi. "Joint optimal power allocation, cooperative beamforming, and jammer selection design to secure untrusted relaying network." *Transactions on Emerging Telecommunications Technologies* 29, no. 3 (2018): e3276.
- [17] Y. Sun, D. W. K. Ng, J. Zhu and R. Schober, "Robust and Secure Resource Allocation for Full-Duplex MISO Multi-carrier NOMA Systems," *in IEEE Transactions on Communications*, vol. 66, no. 9, pp. 4119-4137, Sept. 2018, doi: 10.1109/TCOMM.2018.2830325.
- [18] Y. Li, M. Jiang, Q. Zhang, Q. Li and J. Qin, "Secure Beamforming in Downlink MISO Nonorthogonal Multiple Access Systems," *in IEEE Transactions on Vehicular Technology*, vol. 66, no. 8, pp. 7563-7567, Aug. 2017, doi: 10.1109/TVT.2017.2658563.
- [19] R. M. Corless, G. H. Gonnet, D. E. G. Hare, D. J. Jeffrey, and D. E. Knuth, "On the Lambert W function," *Advances in Computational Mathematics*, vol. 5, no. 1, pp. 329–359, Dec. 1996.
- [20] A. Omri and M. O. Hasna, "Physical Layer Security Analysis of UAV Based Communication Networks," *2018 IEEE 88th Vehicular Technology Conference (VTC-Fall)*, 2018, pp. 1-6, doi: 10.1109/VTCFall.2018.8690950.
- [21] B. Mehlig and J. T. Chalker, "Statistical properties of eigenvectors in non-Hermitian Gaussian random matrix ensembles", *Journal of Mathematical Physics*, 2000, <https://doi.org/10.1063%2F1.533302>.
- [22] B. Clerckx and C. Oestges, *MIMO Wireless Networks: Channels, Techniques and Standards for Multi-Antenna, Multi-User and Multi-Cell Systems*, 2nd ed. Academic Press, 2013.
- [23] D. J. Love, R. W. Heath and T. Strohmer, "Grassmannian beamforming for multiple-input multiple-output wireless systems," *in IEEE Transactions on Information Theory*, vol. 49, no. 10, pp. 2735-2747, Oct. 2003, doi: 10.1109/TIT.2003.817466.
- [24] K. K. Mukkavilli, A. Sabharwal, E. Erkip and B. Aazhang, "On beamforming with finite rate feedback in multiple-antenna systems," *in IEEE Transactions on Information Theory*, vol. 49, no. 10, pp. 2562-2579, Oct. 2003, doi: 10.1109/TIT.2003.817433.
- [25] N. Jindal, "MIMO broadcast channels with finite-rate feedback," *IEEE Trans. Inf. Theory*, vol. 52, no. 11, pp. 5045–5060, Nov. 2006.
- [26] B. Rimoldi and R. Urbanke, "A rate-splitting approach to the Gaussian multiple-access channel," *in IEEE Transactions on Information Theory*, vol. 42, no. 2, pp. 364-375, March 1996, doi: 10.1109/18.485709.
- [27] J. C. Roh and B. D. Rao, "Transmit beamforming in multiple-antenna systems with finite rate feedback: a VQ-based approach," *in IEEE Transactions on Information Theory*, vol. 52, no. 3, pp. 1101-1112, March 2006, doi: 10.1109/TIT.2005.864426.
- [28] W. Wang, K. C. Teh, and K. H. Li, "Secrecy throughput maximization for MISO multi-eavesdropper wiretap channels," *IEEE Trans. Inf. Forensics Security*, vol. 12, no. 3, pp. 505–515, Mar. 2017.
- [29] A. Jeffrey and D. Zwillinger, *Table of Integrals, Series, and Products (6th ed.)*. San Diego, USA: Academic Press, 2000.
- [30] T. Yoo, N. Jindal and A. Goldsmith, "Multi-Antenna Downlink Channels with Limited Feedback and User Selection," *in IEEE Journal on Selected Areas in Communications*, vol. 25, no. 7, pp. 1478-1491, September 2007, doi: 10.1109/JSAC.2007.070920.
- [31] J. Zhang, R. W. Heath, M. Kountouris, and J. G. Andrews, "Mode switching for the multi-antenna broadcast channel based on delay and channel quantization," *EURASIP J. Adv. Sig. Proc.*, vol. 2009, no. 1, p. 802548, Jun. 2009.
- [32] S. Boyd and L. Vandenberghe, *Convex optimization*. Cambridge university press, 2004.
- [33] H. Lei *et al.*, "On Secure Mixed RF-FSO Systems With TAS and Imperfect CSI," *in IEEE Transactions on Communications*, vol. 68, no. 7, pp. 4461-4475, July 2020, doi: 10.1109/TCOMM.2020.2985028.
- [34] H. Bastami, M. Moradikia, H. Behroozi, R. C. de Lamare, A. Abdelhadi, Z. Ding, "Secrecy rate maximization for hardware impaired untrusted relaying network with deep learning", *Phys-*

ical Communication, Volume 49, 2021, 101476, ISSN 1874-4907, <https://doi.org/10.1016/j.phycom.2021.101476>.

- [35] S. Boyd and L. Vandenberghe, *Convex Optimization*. USA: *Cambridge University Press*, 2004.
- [36] D. Bertsekas, *Nonlinear Programming*. Athena Scientific, 1999.